LANGMUIR

pubs.acs.org/Langmuir

Invited Feature Article

Porous Hydrogels: Present Challenges and Future Opportunities

Reza Foudazi, Ryan Zowada, Ica Manas-Zloczower, and Donald L. Feke*

Cite This: https://doi.org/10.1021/acs.langmuir.2c02253

Read Online

ABSTRACT: In this feature article, we critically review the physical properties of porous hydrogels and their production methods. Our main focus is nondense hydrogels that have physical pores besides the space available between adjacent cross-links in the polymer network. After reviewing theories on the kinetics of swelling, equilibrium swelling, the structure−stiffness relationship, and solute diffusion in dense hydrogels, we propose future directions to develop models for porous hydrogels. The aim is to show how porous hydrogels can be designed and produced for studies leading to the modeling of physical properties. Additionally, different methods that are used for making hydrogels with physically incorporated pores are briefly reviewed while discussing the potentials, challenges, and future directions for each method. Among kinetic methods, we discuss bubble generation approaches including reactions, gas injection, phase separation, electrospinning, and freeze-drying. Templating approaches discussed are solid-phase, self-assembled amphiphiles, emulsion, and foam methods.

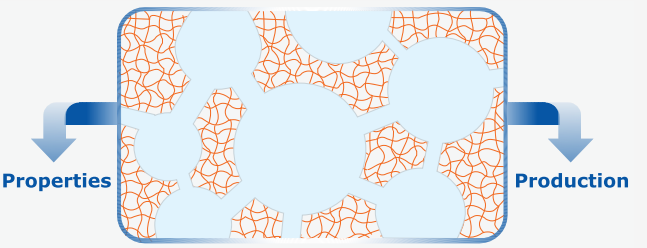

INTRODUCTION

Hydrogels are three-dimensional polymeric networks that have the ability to absorb and maintain high contents of water and aqueous solutions.[1] The presence of networks enables hydrogels to swell in aqueous media without dissolving.[2] Hydrogels can be classified based on the origin of the polymer (i.e., synthetic, natural, or hybrid), composition of the polymer (e.g., homopolymer, copolymer, or composite), the nature of cross-links (i.e., covalent, noncovalent/supramolecular interactions, or combined), the type of networks (i.e., single, semi-interpenetrating, interpenetrating, double network, or mechanically interlocked[3]), the topology of polymer strands between cross-links (linear, graft, branch, etc.), the polymer crystallinity (amorphous or semicrystalline), the charge of the polymeric network (ionic, nonionic, amphoteric, or zwitterionic), the physical appearance (nanoparticles, microparticles, monoliths, films, etc.),[4−6] the functionality (e.g., biodegradability, biocompatibility, stimuli-responsiveness, shape memory, toughness, adhesion, extensibility, self-healing, or superabsorbency),[7−10] and the porosity.[11]

The presence of voids (gas packets) in a solid material (matrix or frame) can significantly change its properties. If voids are more than random trapped air (nominally >5% by volume), then the material is considered to be porous. Porous materials are characterized by the pore-size distribution, the ordered/disordered state of the pore structure, the interconnectivity of pores (closed pore, open pore, or reticulated foams), and the porosity (i.e., the ratio of the void volume fraction to the total volume). The pore size is commonly used to categorize porous materials. The following classification can be found for porous hydrogels in the literature, but we believe this taxonomy should be revised as will be described later:[11,12]

- nonporous hydrogels, which have molecular-sized opening in the network on the order of the macromolecular correlation length, ξ (1−10 nm), also known as mesh size;
- microporous hydrogels (closed pore), having a pore size in the 10−100 nm range;
- macroporous hydrogels having closed pores, usually between 100 nm and 1 μm; and
- superporous hydrogels, which have interconnected pores larger than 100 μm.

It should be noted that hydrogel foams are sometimes classified as a subgroup of macroporous hydrogels containing a percolated network of pores (pore fraction higher than 64 vol %).

The preceding classification ignores the possibility of having open-cell hydrogels with pore size on the order of 10 μm and lower, something that is conveniently accessible by using colloidal templating methods. Additionally, this classification is not consistent with IUPAC's widely accepted definition for porous materials, which does not bind the pore interconnectivity and pore size. In IUPAC's classification, pores are classified

Received: August 19, 2022
Revised: December 29, 2022

https://doi.org/10.1021/acs.langmuir.2c02253
Langmuir XXXX, XXX, XXX−XXX

based on the adsorption mechanisms during standard BET experiment (i.e., N_2 isothermal adsorption at 77 K and 1 atm pressure). Accordingly, macropores are larger than 50 nm and mesopores are in the range of 3.0−50 nm, for which pores show capillary condensation during N_2 adsorption. In this pore classification, micropores are considered to have the size of <1.4 nm, which corresponds to four stacked molecular layers of N_2 (kinetic diameter of N_2 is 0.364 nm).[13]

Hydrogels have molecular-size openings in their network, characterized and reported as the mesh size, defined as the correlation length, ξ_c, or the end-to-end distance of the polymer chain segment between cross-link points also known as the mesh radius, ξ_{rm}.[14] We suggest adapting IUPAC's definition based on water diffusion in hydrogels, considering that the kinetic diameter of a water molecule (0.265 nm) is slightly smaller than that for N_2, and a similar approximation is obtained for the number of molecular-water layers in hydrogel pores. The terminology "dense hydrogel" is sometimes used in the literature for hydrogels without physically incorporated pores and with mesh size on the order of 1−50 nm or so. Therefore, they can be either microporous or mesoporous, depending on the cross-link mesh size. Additionally, materials with pore size smaller than 100 nm are called nanoporous in some publications, suggesting that nanoporous hydrogels can be micro-, meso-, or macroporous. While the term nonporous hydrogel (instead of dense hydrogels) is sometimes used in the literature for hydrogels without any discernible pores, this is terminologically contradictory, considering that hydrogels are defined as materials into which water molecules with 0.265 nm size can easily diffuse. Thus, all swollen hydrogels can be considered as porous materials since they have a mesh or pores, accommodating external molecules. Our proposed taxonomy for porous hydrogels is presented in Table 1.

Table 1. Classification of Hydrogels Based on IUPAC Definitions

Type[a]	Mesh size/physical pore size[b]	Dominant water state[c]
Microporous hydrogels	<1.4 nm	mainly PBW
Supermicroporous hydrogels	1.4−3 nm	PBW and SBW
Mesoporous hydrogels	3−50 nm	PBW, SBW, and FW
Macroporous hydrogels	>50 nm	mainly FW

[a]Porous hydrogels with 1−100 nm pore size have also been labeled as nanoporous. [b]Dense hydrogels are either microporous or mesoporous, depending on the cross-link mesh size. [c]PBW: primary bound water; SBW: secondary bound water; FW: free water.

We classify hydrogels as having closed or open pores, regardless of the interconnection in the network (the space in its network mesh), but rather suggest that the definition of closed or open pores should be based on the significance of capillary action vs diffusivity. In other words, if there are physically interconnected pores that can induce capillary action driven by surface tension, then the hydrogel is classified as open pore. In contrast, if the swelling is controlled by the diffusion of water inside the polymer network or in physically incorporated channels, then the hydrogel is considered to have a closed-cell structure.

Porous hydrogels have several applications in a variety of fields, such as biomaterials,[15−18] drug delivery systems,[19−21] catalysts,[22,23] sensors,[24,25] separation processes (such as adsorbents[26,27] and membranes[28−30]), foods,[31−33] agriculture,[33−37] and additives for concrete.[38] In the next sections, we discuss the physical properties and production methods that incorporate physical pores in hydrogels. In other words, while dense hydrogels have been widely reviewed in different publications, there are few studies that provide an overview of the challenges and opportunities in the production of nondense hydrogels and the fundamental aspects related to their physical properties. Therefore, the main scope of this work is to provide a perspective on nondense hydrogels that have physical pores besides the available space within the strands of the polymer network, as schematically shown in Figure 1.

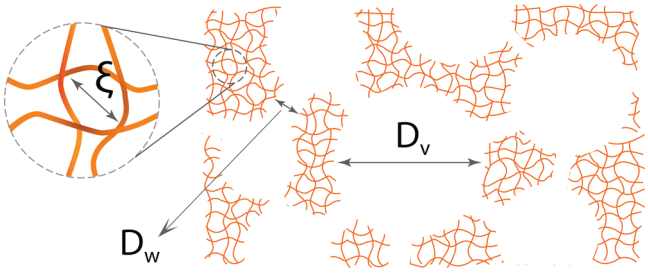

Figure 1. Typical cross-section of a nondense hydrogel, which has an open pore structure: D_v is the pore size, D_w is the size of interconnection between pores, and ξ is the mesh size of the cross-link network.

PHYSICAL PROPERTIES OF HYDROGELS: EXTENSION TO POROUS HYDROGELS

Kinetics of Swelling. Aqueous-based solutions and hydrogel molecules are thermodynamically compatible. However, since the network structure inhibits the dissolution of hydrogels, the diffusion of water molecules with or without solutes into a hydrogel network results in swelling. Most hydrogels are in the glassy state, which makes the kinetics of swelling complicated. As polymer chains are solvated, their behavior changes from a glassy or partially rubbery state to a relaxed rubbery state, which enhances the penetration of solvent molecules within the hydrogel network. Consequently, there is a moving boundary between the unsolvated glassy region and the solvated rubbery phase.[11] The diffusion of water in a dense and glassy polymer of dried hydrogels is very slow. This issue can be resolved by incorporating interconnected pores, which do not completely collapse upon drying (i.e., they are different from the pores created by swelling polymer networks which are characterized by the mesh size).

Two fluid phases (e.g., water and air) within a small capillary tube attain a curved interface, which subsequently induces a pressure difference across the curved interface known as capillary pressure. The Young−Laplace equation relates the capillary pressure P_c to the interfacial tension between two fluids, σ, the effective radius of the tube, r, and the contact angle of the wetting fluid, θ, as $P_c = 2\sigma \cos \theta/r$. Capillary action is significant in porous hydrogels, especially for open-cell macroporous materials due to the hydrophilicity of hydrogels and thus a θ value close to 0. Thus, it can lead to extremely fast swelling due to the enhancement of solvent transport throughout the specimen.[12] Also, incorporating porosity will decrease the thickness of polymer domains, which increases the kinetics of swelling and decreases the time to reach equilibrium.

The swelling ratio of a hydrogel, W, at a given time, t, is defined as follows

https://doi.org/10.1021/acs.langmuir.2c02253
Langmuir XXXX, XXX, XXX−XXX

$$W(t) = \frac{m(t) - m_0}{m_0} \tag{1}$$

where $m(t)$ is the hydrogel mass after being immersed in water for a given time, t, and m_0 is the mass of the dry sample. The state of water in hydrogels plays an important role in their swelling and transport properties. In the first stage of the swelling process, most hydrophilic groups on polymer chains are solvated. The water molecules involved in this step form primary bound water (PBW, also known as strongly bound water). Upon hydration of hydrophilic groups, the polymer network swells, which leads to the exposure of hydrophobic segments of the polymer to the water. The interaction of these hydrophobic segments with water forms secondary bound water (SBW, also known as weakly bound water).[39] The total bound water is defined as the sum of primary and secondary bound water. In the third stage, to minimize the free energy, the osmotic force of the network chains drives additional water into the polymer network. Equilibrium is obtained when the osmotic pressure is balanced by the elastic retraction force of the network. The additional water driven by osmotic pressure is called free water (FW, also known as bulk water), which fills the space between the network chains and larger pores.[39] In nondense hydrogels, the majority of water absorbed via capillary action ends up as FW. Table 1 lists the dominant water states in different porous hydrogels. The bound and free water can be estimated by small molecular probes, differential scanning calorimetry (DSC), or nuclear magnetic resonance (NMR).[39] It should be noted that external conditions, such as pH, temperature, and ionic strength, can influence the water content and swelling ratio.

Since there are no phenomenological models in the literature for the swelling of nondense hydrogels, we first introduce swelling models that have been proposed for dense hydrogels in the next paragraphs. It should be noted that some of these models are not based on a transport mechanism (e.g., kinetics models), thus we will evaluate their applicability in capturing the swelling behavior of nondense hydrogels. In addition, we will discuss the models that have been developed for liquid penetration in nonswelling porous media. Finally, we compare the prediction of presented models with experimental data of both dense and nondense hydrogels with the aim of showing the research gap for the development of new models.

The kinetics of dense hydrogel swelling is controlled by water diffusion within the hydrogel network. For dry polymer networks in the rubbery state, solvent diffusion can be described by a Fickian transport, for which the diffusion coefficient can be corrected by a concentration dependency (also called case I). In this case, the diffusion rate of solvent, R_{diff}, is much lower than the relaxation rate of polymer in the network ($R_{relax} \gg R_{diff}$).[40] However, this model cannot properly predict the swelling of glassy polymers and even polymers close to the glass transition. The kinetics of swelling in such cases can be described by non-Fickian diffusion (case II) when the diffusion rate is much faster than the polymer relaxation rate $R_{diff} \gg R_{relax}$ and as anomalous diffusion when these two processes have similar rates, $R_{diff} \approx R_{relax}$.[40] To determine the mechanism of water diffusion into dense hydrogels, swelling data at early times can be fitted by the following exponential equation

$$\frac{W}{W_\infty} = kt^n \tag{2}$$

where W_∞ is the amount of water absorbed by the hydrogel in the equilibrium state, k is a characteristic constant of the hydrogel, and n is a characteristic exponent of the mode of swelling. For Fickian transport, $n = 0.5$; for anomalous transport, $0.5 < n < 1$; and for case II, $n = 1$.[41] It should be noted that this fitting is usually done for $W/W_\infty \leq 0.6$, where the model assumptions are valid.[42]

Classical kinetics models can also be used to predict the swelling rate of hydrogels, regardless of the porous structure. The first-order kinetics model considers that the swelling rate is proportional to the available swelling capacity, $W_\infty - W$,

$$\frac{dW}{dt} = k(W_\infty - W) \tag{3}$$

where k is the kinetic rate constant. By integration and applying the boundary condition ($W = 0$ at $t = 0$),

$$\ln\left(\frac{W_\infty}{W_\infty - W}\right) = kt \tag{4}$$

It can be shown that the first-order model is aligned with Fick's laws of diffusion for a one-dimensional swelling of hydrogel films. Explicitly, by assuming that the diffusion coefficient, D, of the solvent and the film half-thickness, H, are constant, a one-dimensional swelling of hydrogel films due to the diffusion becomes[43,44]

$$\frac{W_\infty - W}{W_\infty} = \frac{8}{\pi^2}\sum_{i=0}^{\infty}\frac{1}{(2i+1)^2}\exp\left(-\left(\frac{(2i+1)\pi}{H}\right)^2 Dt\right) \tag{5}$$

For long swelling times, only the $i = 0$ term of the summation in this equation is significant, thus

$$\ln\left(\frac{W_\infty}{W_\infty - W}\right) \approx \frac{\pi^2 D}{H^2}t \tag{6}$$

which is an identical form to the first-order kinetics model. When the swelling ratio is significant, the assumption of constant film thickness is not valid. However, since the swelled polymer has enhanced water diffusivity, there is a possibility that the D/H^2 ratio may remain approximately constant, and the first-order kinetics model might sufficiently predict the swelling behavior.[43,45] However, a good fitting may be obtained only in the early and middle stages of swelling. Overall, many hydrogels do not follow a first-order kinetics model, thus a second-order kinetics model (also not a structure-based model) has been proposed[43,45]

$$\frac{dW}{dt} = k(W_\infty - W)^2 \tag{7}$$

which can be integrated by considering $W = 0$ at $t = 0$ and rearranged as follows:

$$\frac{t}{W} = \frac{1}{kW_\infty^{\,2}} + \frac{t}{W_\infty} \tag{8}$$

For long swelling times, the second term on the right-hand side is dominant, which means the slope of a plot of t/W against time approaches $1/W_\infty$ as the swelling reaches equilibrium conditions. Second-order kinetics has been explained in terms of two simultaneous phenomena: the available swelling capacity at time t and the specific interfacial area separating the swollen and unswollen regions.[43] The second-order kinetics model has been found to properly fit the kinetics of water uptake of hydrogels[45] as well as interconnected macroporous polymers with a

https://doi.org/10.1021/acs.langmuir.2c02253
Langmuir XXXX, XXX, XXX−XXX

hydrophobic bulk and hydrophilic pore surface (note that the porous polymer was not a hydrogel in this case).[46] Therefore, this model is a good candidate for understanding the swelling kinetics of porous hydrogels in future studies.

When models for first- or second-order kinetics do not properly describe the swelling behavior, other kinetics models can be evaluated. For example, the kinetics model of a phase-boundary controlled reaction with contracting area has shown the best prediction throughout the isothermal swelling process of poly(acrylic acid) hydrogels in distilled water at different temperatures:

$$1 - \left(\frac{W_\infty - W}{W_\infty}\right)^{1/2} = kt \tag{9}$$

Note that this model predicts a finite time for reaching equilibrium ($t = 1/k$) and is valid only up until that point in time.[47]

The swelling kinetics of hydrogels has also been modeled by using a Voigt viscoelastic model.[48] This model was originally used to describethe creep behavior (i.e., deformation over time) for a viscoelastic material upon application of a constant stress, σ_0:

$$\varepsilon(t) = \frac{\sigma_0}{E}(1 - e^{-t/\tau}) \tag{10}$$

In this equation, the deformation, ε, at time zero is considered to be zero, τ is the retardation time, and E is the Young's modulus. We can elaborate that the swelling process involves the bulk deformation of a solid polymer network (volume change) under a constant external force (i.e., osmotic pressure). The Voigt model can be depicted as a spring and dashpot in parallel, which are assigned to the resistance to expansion of the polymer network and the resistance to permeation during swelling, respectively.[48] Therefore, the creep behavior and swelling of hydrogels are governed by the same phenomenon, and the following equation can be used to model the kinetics of swelling based on eq 10:

$$W = W_\infty(1 - e^{-t/\tau}) \tag{11}$$

The rate of swelling for the Voigt model can be obtained by differentiating the previous equation:

$$\frac{dW}{dt} = \frac{W_\infty}{\tau}e^{-t/\tau} \tag{12}$$

This model has been used to successfully predict the swelling behavior of dense hydrogels.[48,49] To determine the goodness of the model, a linear fit of $\ln(1 - W/W_\infty)$ against time can be evaluated, in which the retardation time is obtained from the slope (i.e., $-1/\tau$). This model predicts a zero intercept for this linear fitting. While a zero intercept is commonly obtained for dense hydrogels when this approach is used, a nonzero intercept is observed for nanoporous hydrogels produced from nanoemulsion templating.[50] The nonzero intercept can be attributed to the fast water uptake through capillary action within the pores.

If we have a porous material (nonhydrogel) in which the swelling of the solid phase is negligible, then the Lucas–Washburn (LW) approach can be used to predict the kinetics of water uptake through capillary action[51,52]

$$m(t) = \sqrt{\frac{c\rho_l^2\sigma\cos\theta}{\eta}t} \Rightarrow W = S\sqrt{t} \tag{13}$$

where m is the mass (kg) of fluid infiltrating the porous material, c is the capillary constant (m^4) of the porous material, η is the viscosity (Pa·s) of the penetrating fluid, ρ_l is the density (kg·m^{-3}) of the penetrating fluid, σ is the interfacial tension (N·m^{-1}) of the fluid, t is time (s), and θ is the contact angle between the penetrating fluid and porous material. The right-side equation is a simplification of the LW equation used for linear fitting of the data, in which S shows the sorptivity. The equation has two unknown parameters: c and θ. However, if the surface of the pores is very hydrophilic (as in hydrogels), then the water contact angle will be very low (i.e., $\theta \approx 0$) and c can be found. Note that this equation does not consider the swelling of the polymer phase in the hydrogels.

A linear fitting of W vs $t^{1/2}$ frequently shows a nonzero intercept, which can be attributed to the rapid filling of surface pores.[53] Additionally, deviations from linearity in fitting W vs $t^{1/2}$ data could result from the retarding effect of gravity on vertical capillary action[53] or the interaction of solutes present in the aqueous media with the pore surface.[51] The $W \approx t^{1/2}$ scaling in eq 13 can be extended to $W \approx t^{1/2D_T}$, where D_T is the fractal dimension of the pore structure and is equal to 1 for straight pores, between 1 and 2 for two-dimensionally distributed pores, and between 2 and 3 for three-dimensional porous spaces.[53] It should be noted that this equation has the same scaling with time as eq 2 for Fickian diffusion. Thus, if an open-cell porous hydrogel shows the same scaling behavior of fluid uptake with time, it will be difficult to determine whether the Fickian diffusion or LW-controlled capillary action is dominant. A deviation from $W \approx t^{1/2}$ scaling in open-cell hydrogels should conservatively be interpreted as a non-Fickian diffusion in the polymer phase when the exponent is higher than 0.5 and may be attributed to tortuosity in the porous structure when the exponent is lower than 0.5.

A summary of models is presented in Table 2. To evaluate and compare the models reviewed in this section, we present the swelling data for dense hydrogels as well as open-cell macroporous hydrogels synthesized by high internal phase emulsion (HIPE) and foam templating methods with different

Table 2. Summary of Models Available for Predicting the Water Uptake of Porous Hydrogels

Model	Equation	Limitations/Assumptions
Fickian transport and Lucas–Washburn	$W = c_0 t^{1/2}$	early uptake/penetration
modified Lucas-Washburn	$W = c_0 t^{1/2\,D_T}$	early uptake/penetration
anomalous transport	$W/W_\infty = kt^n$,where $0.5 < n < 1$	$W/W_\infty \leq 0.6$
case II	$W/W_\infty = kt^n$	$W/W_\infty \leq 0.6$
first-order kinetics	$\ln(W_\infty/W_\infty - W) = kt$	proportionality of the swelling rate and the available swelling capacity
second-order kinetics	$t/W = 1/kW_\infty^2 + t/W_\infty$	unestablished physical meaning
phase-boundary controlled kinetics	$1 - [(W_\infty - W/)W_\infty]^{1/2} = kt$	valid up to $t = 1/k$, when equilibrium is reached
Voigt	$W = W_\infty(1 - e^{-t/\tau})$	improper fitting when water uptake is fast due to capillary action

https://doi.org/10.1021/acs.langmuir.2c02253
Langmuir XXXX, XXX, XXX−XXX

pore sizes in the range of 9−130 μm. The maximum water holding capacity of macroporous hydrogels is over 4000 wt %.[54] All hydrogels have the same monomer (2-acrylamido-2-methyl-1-propanesulfonic acid, AMPS), cross-linker (*N*,*N*′-methylene-(bis)acrylamide, MBA), and monomer to cross-linker ratio, 10:1.[54] As seen in Figure 2, all hydrogels (dense and nondense in this broad pore size and interconnectivity range) can properly be fitted only by the second-order kinetics model.

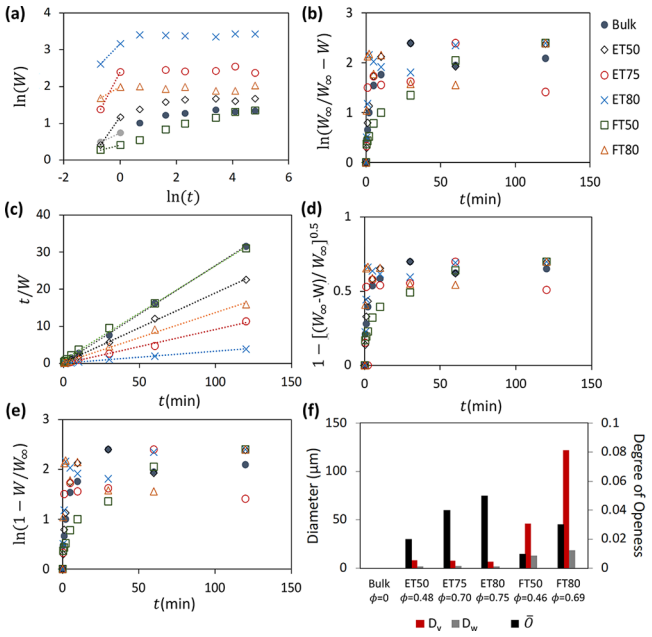

Figure 2. Evaluation of models for the water uptake of macroporous hydrogels prepared via emulsion templating (ET) and foam templating (FT) methods. The swelling behavior of the dense hydrogel (indicated as a bulk sample) with the same chemistry is also provided for comparison. The number after ET/FT shows the templated porosity, which can be different from the final porosity of the hydrogels (e.g., compare the templated volume fraction of pores with the actual porosity of ET and FT samples shown by ϕ below sample names in (f)). Fitting of eq 2 at low swelling rates is shown in (a). The slope of the data is different from 0.5 except for dense hydrogel, which means that the simple LW approach, eq 13, cannot explain the capillary action. The results shown in (b), (d), and (e) are plotted according to eqs 4, 9, and 11 for linear fittings, respectively, but a linear dependence is not observed for any specimens. Plot (c) shows the fitting of the second-order kinetics model, with $R^2 \geq 0.99$. The pore size, D_v, size of interconnection between pores, D_w, and degree of openness, $\bar{O}$, for studied samples in (a−e) are summarized in (f). Data are from Zowada et al.[54]

The results in Figure 2 show that there is a need for developing new models that can predict the water uptake of porous hydrogels. These models should relate the water uptake to the nature of the polymer phase, the porosity, pore size distribution, and interconnectivity of the porous hydrogel. While the second-order kinetics model well predicts the behavior of several different dense and nondense hydrogels, it is a semiempirical model. Future work may establish a theoretical background and fundamental basis for correlating the kinetics model constants and the structural parameters of the porous hydrogel (e.g., the Flory−Huggins polymer−solvent interaction parameter, porosity, pore-size distribution, and interconnectivity of the porous hydrogel). Another challenge in porous hydrogels is that the swelling of the polymer phase and capillary action of pores take place simultaneously; therefore, separating their effect on water uptake is not straightforward. Future studies should perform control experiments using solvents that induce minimal swelling in the polymer phase so that the effect of capillary action can be distinguished from swelling of the polymer phase.

Equilibrium Swelling Capacity. The key component in the hydrogel swelling capacity is its cross-link structure. If polymer chains are not cross-linked (physically and/or chemically), then they will eventually dissolve when immersed in the solvent. Note that a poor solvent can swell a polymer without chemical cross-links but may not dissolve it if the physical interactions between polymer chains cannot be overcome. In this case, the interactions between polymer chains induce physical cross-links. Obviously, the main solvent in the hydrogel literature is water, which mostly interacts through hydrogen bonding with polymer chains in this case. However, the swelling capacity in other solvents (e.g., solvents that do not form hydrogen bonds with hydrogel chains) can be used to determine the contributions of physical and chemical cross-links to the network properties.[55]

Similar to the swelling kinetics behavior, there is no phenomenological model in the literature for the equilibrium swelling of hydrogels with physically incorporated pores. Thus, we first introduce models that have been proposed for dense hydrogels, eqs 14 and 15). Then, we will discuss how the amount of water entrapped in pores can be subtracted in nondense hydrogels. Therefore, the equilibrium swelling of the polymer phase in nondense hydrogels can be determined and used for the calculation of network characteristics with these equations.

The equilibrium swelling of hydrogels is controlled by the network structure, cross-link density, and average molecular weight of polymer between cross-links in the network. There are three states that are considered for modeling the swelling: dried, relaxed, and swollen states. Since usually hydrogels are formed by the polymerization of monomers in the presence of water, the relaxed state is assumed to be the network structure obtained immediately after cross-linking. In the relaxed state, there is no force propagating through the network.[56,57] The formed network can incorporate additional water until reaching the equilibrium state (i.e., maximum swelling).

The equilibrium swelling can be modeled thermodynamically by evaluating the effects of water addition to a hydrogel network. The first equilibrium swelling model was proposed by Flory and Rehner by considering the entropic contribution of mixing polymer with solvent, which is balanced by the elastic energy of the swollen polymer network containing additional solvent[58,59]

$$\frac{1}{\bar{M}_c} = \frac{2}{\bar{M}_n} - \frac{\ln(1-\phi_s) + \phi_s + \chi\phi_s^2}{V_1\rho_d(\phi_s^{1/3} - \phi_s/2)} \quad (14)$$

where $\bar{M}_c$ is the number-average molecular weight between cross-links in the polymer network, $\bar{M}_n$ is the average molecular weight of the polymer chains prior to cross-linking, ϕ_s is the polymer volume fraction in the swollen equilibrium state, χ is the polymer−solvent interaction parameter, V_1 is the molar volume of the solvent, and ρ_d is the dry density of the polymer network. It should be noted that the χ parameter is an average of noncovalent and nonionic interactions between the polymer and solvent. The interaction parameter changes with polymer volume fraction due to the reduced affinity between polymer and solvent upon cross-linking. Therefore, it should be corrected for cross-link and volume-fraction dependencies.[60]

https://doi.org/10.1021/acs.langmuir.2c02253
Langmuir XXXX, XXX, XXX−XXX

Richbourg and Peppas discussed how the Flory–Rehner model can be extended to pH-dependent swelling of weakly ionic hydrogels[61]

$$\bar{M}_c = -\frac{\left(1-\frac{2}{f}\right)(1-\Gamma)V_1\rho_d\phi_r^{2/3}\phi_s^{1/3}}{\ln(1-\phi_s)+\phi_s+\chi\phi_s^2+2V_1\left(I-\sqrt{I^2+\left(\frac{i\phi_s\rho_d}{2M_r}\right)^2}\right)} \quad (15)$$

where f is the junction functionality (the number of chains connected to a cross-link node) in a polymer network, Γ is the frequency of chain-end defects, ϕ_r is the polymer volume fraction in the relaxed state, I is the ionic strength, i is the degree of ionization of the polymer repeat unit (note that for neutral polymers, $i = 0$), and M_r is the molecular weight of the polymer repeat unit. The first two terms in the numerator of the right-hand side, $(1 - 2/f)$ and $(1 - \Gamma)$, correct nontetrafunctional networks and network imperfections, respectively. For chemical cross-links, the value of f can be approximated from the chemistry (by neglecting the possibility of different f values for the physical cross-links in the same system). A similar approximation can be made to estimate Γ from the stoichiometry of functional groups participating in the cross-linking scheme. When $I = 0$ and $i = 0$ (e.g., swelling of a neutral hydrogel in deionized water), a modified version of the Flory–Rehner equation is obtained in which network imperfections and nontetrafunctional networks are taken into account.

The equilibrium water uptake of hydrogels significantly increases by inducing greater porosity in their structure. While the water absorbed by dense hydrogels can be in the form of primary bound water, weakly bound water, and free water, the water in the pores of mesoporous and macroporous hydrogels is free water with minimal interaction with polymer chains. Therefore, to estimate the polymer network parameters of these porous hydrogels from equilibrium swelling models, the water uptake by pores should be excluded. To subtract the water content of pores from the total water uptake of mesoporous and macroporous hydrogels, one should consider that the swelling of a porous hydrogel can change the pore volume fraction,[50] which takes place to accommodate the increase in the swollen polymer phase. To estimate the change in the pore volume fraction, one can test a control dense hydrogel with the same polymer composition as the polymer domain of porous hydrogels in which a few visually measurable pores are incorporated.[50] Alternatively, a simple estimation can be made by assuming that the swelling of the polymer phase is affine and takes place equally in three dimensions; therefore, the pore volume decreases upon swelling proportional to the change in volume of the polymer phase of the hydrogel. However, this approximation is applicable only to small swelling ratios because this method predicts a complete disappearance of pores for swelling ratios higher than the reciprocal of the pore volume fraction (i.e., $1/\phi_{pore}$), which has not been reported so far.

One finding that deserves to be further evaluated is the effect of the pore formation process on the network structure of the polymer phase. For example, our recent study shows that the polymer network is influenced by the pore packing in porous hydrogels which have been produced through an emulsion templating method.[50] In other words, while the samples have the same porosity and pore size, they show different swelling kinetics and equilibrium swelling for different packing of pores.[50]

Structure–Stiffness Relationship. The rubber elasticity model relates the stiffness of a swollen dense hydrogel to the entropy loss due to the extension of polymer chains in the network. For hydrogels highly swollen with water, the phantom network model developed by James and Guth[62] provides a better approximation than the affine network model suggested by Flory and Rehner.[58,59] The former assumes that junctions move independently of chains, whereas the latter considers the movement of junctions proportional to the macroscopic deformation. The original model assumes that the shear modulus, G, of the swollen hydrogel is related to the number of chains in the polymer network υ[63]

$$G = \upsilon RT \quad (16)$$

where R is the ideal gas constant and T is the temperature. However, the model should be corrected for swollen polymer networks, nontetrafunctional networks, and network imperfections:[61]

$$G = RT\left(1-\frac{2}{f}\right)(1-\Gamma)\frac{\rho_d}{\bar{M}_c}\phi_r^{2/3}\phi_s^{1/3} \quad (17)$$

Among these parameters, ρ_d, ϕ_r, and ϕ_s are determined straightforwardly, whereas f and Γ can be approximated from the chemistry as described in the previous section. Thus, the value of $\bar{M}_c$ can be estimated. This model has some limitations since it ignores the effects of polymer chain stiffness, the chain length distribution between cross-links, and higher-order bonding. Consequently, the estimation of $\bar{M}_c$ by using rubber-elasticity theory involves some systematic errors.[61]

For mesoporous and microporous hydrogels where the contribution of free water becomes significant, the prediction of hydrogel structure from this model involves significant errors. By assuming negligible contributions from the water phase to the mechanical properties, we suggest that the simplest remedy for this miscalculation is to correct the shear modulus with either isostrain (upper bound) or isostress (lower bound) mixing rules, respectively:

$$G_{isostrain} = (1-\phi_{pore})G \quad (18a)$$

$$G_{isostress} = \frac{1}{1-\phi_{pore}}G \quad (18b)$$

$G_{isostrain}$ and $G_{isostress}$ are the measured shear moduli of the porous hydrogels, which are used to estimate the G value of the swollen polymer phase. However, systematic studies are needed to determine which correction provides a more realistic prediction. The corrected shear modulus, G, can then be used in eq 17 to determine the structural parameters of the polymer network.

Hydrogels have both solid and liquid phases; therefore, they are not pure elastic materials and have time-dependent behavior. Two approaches are usually considered for materials having both solid and fluid phases: viscoelasticity and poroelasticity.[64] The viscoelastic behavior of hydrogels can be described by common models, such as the Maxwell, generalized Maxwell, Kelvin–Voigt, and four-element models. To measure the viscoelastic behavior of hydrogels, small-amplitude oscillatory shear (SAOS) experiments can be performed. In these experiments, the hydrogels undergo a sinusoidal strain ($\gamma = \gamma_0 \sin \omega t$, where γ_0 and t are the maximum strain amplitude and time, respectively) at an angular frequency of ω. The viscoelastic

https://doi.org/10.1021/acs.langmuir.2c02253
Langmuir XXXX, XXX, XXX–XXX

hydrogels will respond with an out-of-phase sinusoidal stress (σ), from which the storage and loss moduli are defined

$$\sigma = \gamma_0[G'(\omega)\sin \omega t + G''(\omega)\cos \omega t] \tag{19}$$

where $G'(\omega)$ is the frequency-dependent storage modulus and $G''(\omega)$ is the frequency-dependent loss modulus, which are independent of the strain amplitude. The former shows the elastic response, whereas the latter is an indication of the viscous behavior of the hydrogels. The tangent of the phase angle, which provides a measure of damping, is defined as follows:

$$\tan \delta = \frac{G''}{G'} \tag{20}$$

From this equation, a tan δ value that is close to zero indicates solid-like behavior (note that for $\delta = 0$, stress and strain are in phase), and tan δ higher than 1 shows liquid-like behavior (note that for $\delta = 90°$, stress and strain are completely out of phase). Hydrogels usually exhibit solid-like behavior and tan δ values close to zero. The viscoelastic measurements of hydrogels mostly show a plateau in G' in the 0.01−100 Hz frequency range and a minimum in G'' in the mid-frequency of this range. In other words, they are in the rubbery zone of general viscoelastic behavior. Consequently, determining the relaxation times from fitting viscoelastic models involves errors (i.e., the relaxation time may be estimated from extrapolation only if a $G' - G''$ crossover is not apparent). In addition, the G'' minimum shows a change in relaxation mechanism from the network level (low frequencies) to segmental level of the network (high frequencies).[18,65]

For estimating the structural parameters from eq 16 or 17, the shear modulus of hydrogels is commonly estimated from the storage modulus in the linear viscoelastic regime due to their solid-like behavior. There are very limited reports of models correlating the structure and viscoelastic parameters of hydrogels or even experimental viscoelastic measurements on hydrogels with carefully designed structures. The challenge to perform such studies as future work is to produce porous hydrogels with designed porosity and interconnectivity, which can be addressed by methods summarized in the next sections.

Another advanced approach to modeling the mechanical properties of porous hydrogels is to employ poroelastic (also called biphasic) constitutive equations. In poroelastic models, the contributions of fluid flow through pores are also considered in the stress−strain behavior under deformation. Biot was a pioneer in establishing poroelasticity,[66] which has been developed for hydrogels since then.[67−70] The most important parameters that control the poroelasticity of hydrogels are the elastic modulus of the solid (polymer) phase, the Poisson's ratio of dried and swollen hydrogels, fluid−solid interactions, intrinsic permeability, and viscosity of the solvent (which is water for hydrogels).[64]

Indentation techniques have been widely used to simplify the poroelastic characterization of hydrogels,[67,68] which still require complicated numerical simulations[70,71] or at best can be approximated by linear poroelasticity at small deformations.[66] By digging into the literature, one can identify some macroporous hydrogels from the authors' description of synthesis approaches and the physical appearance of the hydrogels, for which poroelastic studies have been performed.[70] We believe the future direction for correlation between the structure and stiffness of porous hydrogels is to further expand studies on poroelasticity and poroviscoelasticity. In particular, there are challenges to decoupling the characteristic times associated with the poroelasticity (mainly controlled by intrinsic permeability) and viscoelasticity (mainly controlled by the relaxation of swollen polymer chains) of hydrogels[69] and evaluating the structure−stiffness relationship in relaxed/unrelaxed states of poroelasticity and viscoelasticity.[71] For functional hydrogels such as self-healing ones, there is a lack of study on the correlation of mechanical-property evolution with porous and molecular structures.

Solute Diffusion in Hydrogels. Mesh-size theory estimates the reduction in solute diffusivity due to physical interactions of a solute with a polymer chain and the mesh size of the network, ξ. The mesh size, which represents the distance between two connected junctions, is the average correlation length of a chain in the swollen hydrogel. ξ determines if the solute can pass through the space between polymer chains in the network. This model assumes that the chemical potential gradient, convective flow, and solute−polymer binding within a homogeneous hydrogel are not significant, thus the transport is described by the effective diffusivity. The mesh size can be measured by correlation techniques, including swelling data as proposed by Canal and Peppas[72]

$$\xi = \phi_s^{-1/3}\left(l^2 C_n \frac{2\bar{M}_c}{M_r}\right)^{1/2} \tag{21}$$

where l is the carbon−carbon bond length in the polymer and C_n is the characteristic ratio for a polymer chain of n repeat units. This equation was developed for vinyl polymers, so the 2 in the equation accounts for two carbon−carbon bonds per repeat unit. This model has been improved by converting it from an affine model to a phantom network model, assuming chains are long enough to have a Gaussian distribution, and using a backbone bond factor, λ, instead of a vinyl-specific prefactor[61]

$$\xi = \phi_s^{-1/3}\left(\left(1 - \frac{2}{f}\right)\bar{l}^2 C_\infty \frac{\lambda \bar{M}_c}{M_r}\right)^{1/2} \tag{22}$$

where $\bar{l}$ is the weighted average of the bond lengths per repeat unit and C_∞ is the characteristic ratio for a long polymer chain.

The Stokes−Einstein equation can be used to determine the diffusion coefficient of a solute in the solvent in the absence of convective flow

$$D_0 = \frac{k_B T}{6\pi\eta r_s} \tag{23}$$

where η is the solvent viscosity, r_s is the effective radius of the solute molecules, k_B is the Boltzmann constant, and T is the temperature. Two models have been developed to determine the change in the diffusivity of solute, D, within the hydrogel network, the free volume model[73,74] and the competing-obstruction scaling model,[75] which are as follows, respectively,

$$\frac{D}{D_0} \approx \left(1 - \frac{r_s}{\xi}\right)\exp\left(-\frac{\phi}{1-\phi}\right) \tag{24a}$$

$$\frac{D}{D_0} = \exp\left(-\frac{r_s + r_f}{r_f}\phi^{1/2}\right) \tag{24b}$$

where ϕ is the polymer volume fraction in the hydrogel and r_f is the radius of polymer fibers in the hydrogel network. The current mesh-size theories do not consider the effects of solute shape, free-volume void spaces, and the mesh openings.[61]

https://doi.org/10.1021/acs.langmuir.2c02253
Langmuir XXXX, XXX, XXX−XXX

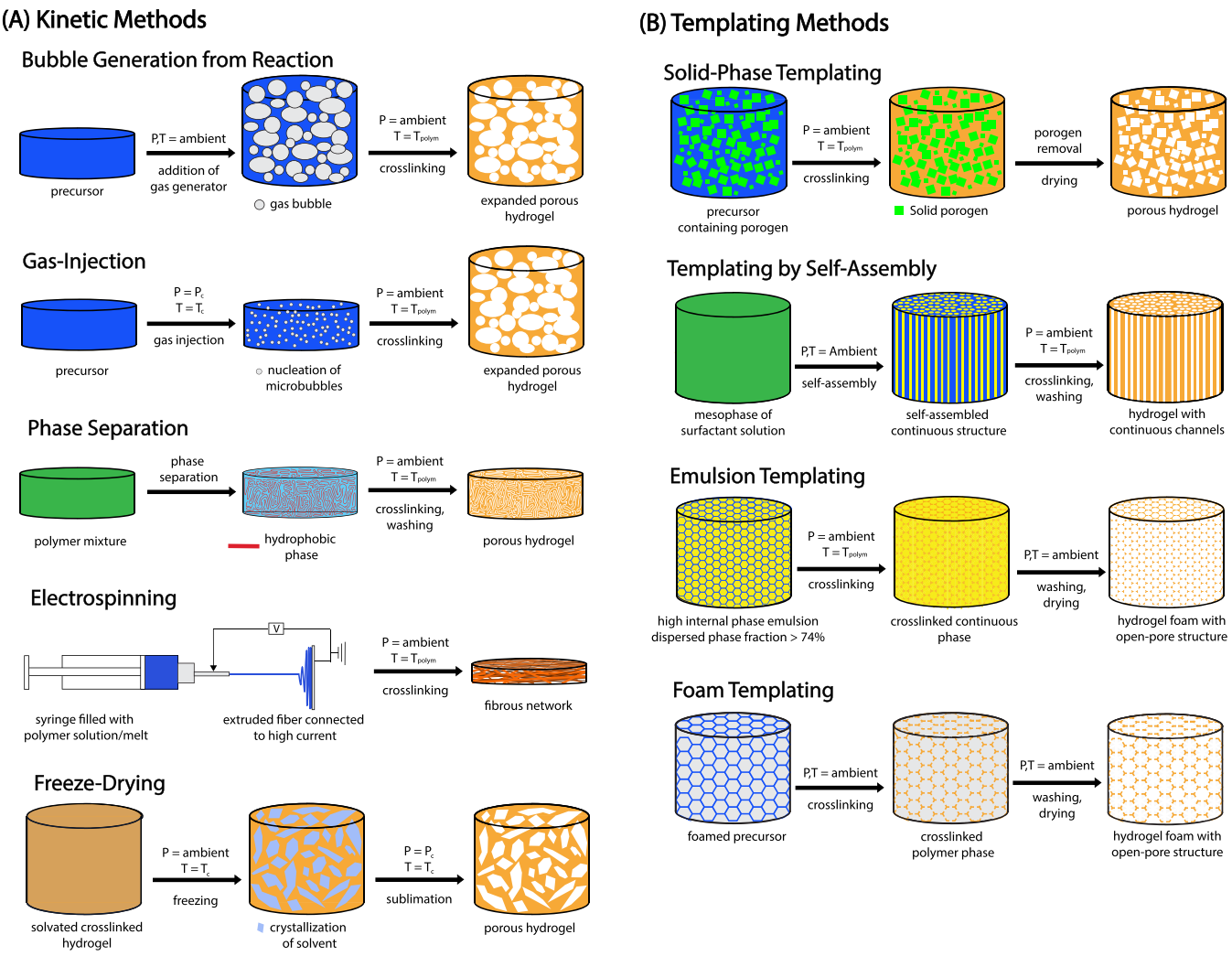

Figure 3. Different methods for the production of porous hydrogels, classified as templating and kinetic methods.

The diffusion of solutes in the pores of mesoporous and macroporous hydrogels, which contain free water, can be modeled as diffusion in porous media.[76] However, this approach has not received enough attention. Saying that, one should note that the solute diffusion in hydrogels is intended for controlled delivery applications (i.e., solutes are incorporated into the polymer network and will be released slowly as the hydrogel is placed in contact with the target environment). If pores beyond the mesh size of the polymer network are incorporated, then the diffusion of solute will be enhanced; therefore, the range of controlled release rates will be broadened. A potential area for future work is to provide a multimode diffusion model including the diffusion within both the polymer network (e.g., as in eqs 24a and 24b) and the interconnected mesoporous or macroporous network. The hypothesis here is that the closed pores in hydrogels have an insignificant effect on the solute diffusion in hydrogels. There will be a need for experimental studies to confirm this hypothesis.

PRODUCTION OF POROUS HYDROGELS

Basics. *Fabrication Methods.* Further development of models for the physical properties of porous hydrogels requires more experimental studies on hydrogels with different porous structure. In the next sections, therefore, different methods that are used for making hydrogels with physically incorporated pores are briefly reviewed and the potentials, challenges, and future direction for each method are discussed. The aim is to show how porous hydrogels can be designed and produced for systematic studies on modeling their physical properties. Production methods can be classified as either kinetic or templating approaches (Figure 3). Frequently used kinetic methods are bubble generation from reaction, gas injection, phase separation, electrospinning, and freeze-drying methods. In these methods, the microstructure of the system is dynamically evolving until it is arrested. In templating methods, the porous polymer is a replicate of the original template. The challenge in kinetic methods is to control the porosity and pore size independently, whereas the retention of templated structure in templating methods may not always be straightforward.

Air-in-Liquid Dispersions. Techniques involving bubble generation from reaction, gas injection, and foam-templating methods have an intermediate stage where air is dispersed in a liquid phase. The classification of air-in-liquid dispersions is based on the liquid volume fraction, ϕ. If $\phi < 0.05$, then the dispersion is considered a "dry foam"; if $\phi < \phi_c$ (where $\phi_c = 0.36$ for polydisperse foams), then we have a "wet foam"; and a dispersion with $\phi > \phi_c$ is a "bubbly liquid".[77] Most reported cases using these methods in the literature have dealt with wet foams and bubbly liquids. To obtain an open-pore cellular polymer, the dry foam and wet foam dispersions are of interest,

https://doi.org/10.1021/acs.langmuir.2c02253
Langmuir XXXX, XXX, XXX−XXX

whereas a closed-pore cellular polymer is very likely if the intermediate stage is a bubbly liquid. However, it should be noted that the air−liquid interfacial properties play a significant role. In other words, there are cases that the liquid volume fraction is low but a closed-pore cellular polymer is obtained. As discussed recently, the formation of interconnections between pores in a porous polymer is controlled by the depletion-induced drainage of the interdroplet/interbubble layer[78] (also known as a foam film in the foam literature).

Nucleation and Growth Mechanisms. Another important phenomenon in making porous hydrogels through gas generation or injection is the nucleation and growth of bubbles. At low concentrations and/or high pressures, the gas is dissolved in the liquid phase. The first stage of phase separation of dissolved gas from liquid is nucleation, in which the density and energy fluctuations in a metastable system lead to the formation of microbubbles. Microbubbles, which may diminish or grow, are submicrometer-sized bubbles originating from the clustering of gas molecules. The critical nuclei size is the minimum microbubble size above which the nuclei are thermodynamically stable, meaning that the Gibbs free energy of having a gas phase dominates the energy required to form new interfaces. It should be noted that in the presence of phase boundaries (e.g., impurities and surfaces), heterogeneous nucleation takes place.[79,80] Since the phase boundaries decrease the barrier for the formation of new interfaces, heterogeneous nucleation is more common than homogeneous. After the nucleation of microbubbles, their growth kinetics will be governed by several physical factors, such as gas mass transfer, elongational viscosity, viscoelasticity, and bubble−bubble interactions.[80−83] However, these factors have not been comprehensively studied for pore formation with different gases in porous hydrogel synthesis. Additionally, considering that there is a strong move toward the addition of nanoparticles to hydrogels to improve the mechanical properties or incorporate certain functionalities,[18] one of the current challenges is how to control or exploit the effect of shape and size distributions of nanoparticles on the nucleation process.

Stability of Liquid Foams. The stability of wet foams is mainly controlled by Ostwald ripening, drainage, and coalescence. As the bubble size in foams is not commonly monodisperse, the difference in Laplace pressure between bubbles (as well as with external atmospheric air) can induce Ostwald ripening, in which the gas in smaller droplets is driven toward larger bubbles or the external atmosphere. The solubility of gas in the continuous phase controls Ostwald ripening. If a porous hydrogel precursor undergoes Ostwald ripening, then the bubble size increases with time with $d \approx t^{1/3}$ scaling.[84] Since Ostwald ripening intensifies as the temperature is increased,[85] the pore size increase becomes more significant upon polymerization at high temperatures and for exothermic polymerization reactions. The other mechanism of instability is coalescence, in which the film between bubbles undergoes drainage and subsequent rupture. If coalescence is dominant in a porous hydrogel precursor, then the bubble size increases with time with $d \approx t^{1/2}$ scaling. It should be noted that creaming instability is also possible in a dispersion of bubbles due to the density difference of the continuous and dispersed phases inducing the drainage of the liquid phase. However, creaming can also be exploited to produce porous hydrogels with a gradient in porosity.

Bubble Generation from Reaction. One of the techniques used to form pores in polymers is to generate a gas phase upon polymerization or other side reactions. The classical example of this method is polyurethane (PU) foams, in which a small amount of water reacts with isocyanate groups of the monomers to generate CO_2 gas.[86] Consequently, the polymer contains both urethane and urea groups in the chain, where the latter can phase separate to form hard segments. The competition between the kinetics of polymerization and the CO_2 formation and diffusion controls the morphology of the final polymer. If the former is much faster than the latter, then a closed-cell PU foam with low porosity is obtained. The opposite scenario will result in the foam collapses before solidification. Clearly, these two processes can be adjusted to produce open-pore PU foams with controlled interconnectivity. However, the degree of interconnectivity will not be independent of pore density. This is a major challenge with most of the nontemplating methods. The chemistry of polyurethane can be adjusted to make them hydrophilic and suitable for hydrogel applications. Another system in which the polymerizing phase is also involved in the formation of the gas phase is the polymerization of acidic monomers, such as acrylic acid and AMPS, in the presence of metal carbonates.[12]

Gas generation can also be achieved by side reactions through thermal or chemical decomposition. The chemicals that are used to induce gas-generation reactions are called blowing agents (e.g., water is the blowing agent in PU foams). The major gas products from chemical blowing agents are as follows:[87]

- CO_2 (e.g., sodium bicarbonate reaction with acids and thermal decomposition of zinc carbonate);
- H_2 (e.g., sodium borohydride reaction with water and magnesium hydride reaction with water);
- O_2 (e.g., decomposition of hydrogen peroxide); and
- N_2 (e.g., decomposition of azo-compounds and hydrazine derivatives).

Similar to PU foam synthesis, gas generation by side reactions usually takes place during polymerization or cross-linking of the hydrogel, so the bubbles are trapped more efficiently by the increasing viscosity. The bubble formation undergoes a nucleation and growth process, which will be effectively suppressed when the 3D network forms in the polymer phase. Usually, the reported pore sizes range from 50 to 1000 μm and porosity varies between 35 and 85% depending on the system and additive.[4] There are many parameters in these systems that affect the initial and final foam structure such as the additive (e.g., to enhance the nucleation or to stabilize the formed bubbles), rate of gas generation, rate of cross-linking, and foam stability. The generated gas will lead to bubble formation and consequently foaming if it undergoes a phase separation from the liquid cross-linking medium. In other words, if the generated gas has high solubility in the polymerizing phase, then a porous hydrogel may not form.

Since hydrogel synthesis often takes place in aqueous media, the gas solubility in water can play a detrimental role. Among commonly generated gases, CO_2 has higher solubility than N_2 in water, thus the liquid foam of CO_2 coarsens faster due to enhanced Ostwald ripening, generating larger pore sizes under similar conditions. Also, high solubility can suppress the nucleation in the liquid phase, resulting in limited bubble formation and insufficient imbedded porosity. As expected, the chemistry of components in the aqueous media, most importantly monomers and polymers, influences the solubility and bubble nucleation of generated gas. However, the thermodynamics (solubility and diffusivity of gas in hydrogel precursors) and kinetics (nucleation and growth of bubbles) of

https://doi.org/10.1021/acs.langmuir.2c02253
Langmuir XXXX, XXX, XXX−XXX

such a complicated system have not been studied. A technical challenge is the limited solubility of many chemical blowing agents in aqueous media (e.g., azodicarbonamide). Also, when a thermally activated blowing agent is used in producing hydrogels from water-based precursors, one should consider that water can be lost due to evaporation and the stability of foam usually decreases as the temperature is increased.

Bubble growth is affected by the elongational rheology of the continuous phase and the interfacial rheology. For example, surfactants can be included in the hydrogel precursor to stabilize generated bubbles and decrease the dissolution of the gas phase, or thickeners can be added to enhance the elongational viscosity. However, there is a lack of reliable data on the evolution of these properties as the polymerization progresses and their effect on the structure of the porous hydrogel produced.

Bubble generation from reaction is an economical method in terms of energy and material. It does not require specialized equipment, and the porosity can be created via reaction rather than a sacrificial template. This is a favorable method for specific applications such as tissue engineering because it minimizes the use of toxic chemicals and solvents and reduces the necessity of removing artifacts of the templating process. The main disadvantages with this method is that the pore size and porosity are difficult to control and have unreliable reproducibility since they are generated via reaction.[88] The main approach in controlling the structure is the cross-linking rate of the polymer solution which already needs to be rapid in order to preserve the unstable foam structure. The pores can be extremely polydisperse, and interconnectivity can be achieved only at high porosities due to high liquid−air interfacial tension. There can also be a pore-size gradient within the resulting hydrogel due to the creaming instability. The reaction kinetics of the polymer phase needs to be considered as the primary tool for controlling this instability.

Gas Injection in Polymer Melt or Precursor. Instead of generating gas from a reaction, a gas phase can be injected in a polymer or polymer precursor. The injected gas is known as a physical blowing agent, which can be injected under pressure and expands upon reducing pressure. Alternately, low-boiling-point liquids can be used. Examples of the former are CO_2 and butane, whereas short aliphatic chain molecules and hydrofluoroolefins are commonly used in the latter case.[87] The low cost and nontoxicity of CO_2 have made it a favorite physical blowing agent. We distinguish this method from foam templating in which bubbles are entrapped in the precursor by agitation, frothing, insufflating, or similar constant-pressure manufacturing. This classification is based on the mechanism of bubble formation. The key elements in forming porous polymers by gas injection are (1) the dissolution of gas in the liquid/melt under high pressure and/or low temperature and (2) reaching supersaturation by decreasing pressure or increasing temperature, after which (3) nucleation and growth take place.[89,90] The porous structure is stabilized either by reaching a glassy state (note that gas dissolution can lower the glass-transition temperature of polymers and make them rubbery) or the formation of a network. However, the former is more common, and there is a lack of comprehensive studies on the latter case. While gas solubility in the liquid phase is essential in this method, the high gas solubility can suppress foaming or destabilize the foaming in the bubble generation from reaction (described in a previous section). Therefore, these two methods are put into two separate classes.

While the gas injection method is industrially used to prepare polyolefin foams, its use to prepare porous hydrogels is not common. The main challenge is that among gases, even CO_2 has low solubility in hydrophilic polymers and prepolymers (i.e., high solubility is essential to achieveing high porosity).[91] A solution for this challenge is to use a cosolvent to enhance the solubility and thus subsequently form pores. To avoid concerns related to organic cosolvents, more studies on ionic liquids can be envisioned.[92] Another solution to overcoming the challenges of foaming hydrogels through gas injection is to use supercritical CO_2 (sc-CO_2), which has gas-like viscosity and liquid-like density and can be easily obtained under conditions above T_c = 31 °C and P_c = 7.38 MPa. Although supercritical conditions for CO_2 can be achieved with current polymer processing equipment, foaming of hydrogels with sc-CO_2 is still not economical. The main drawbacks of the gas injection method are that the interconnectivity between pores is limited (approximately 10−30% of pores are interconnected)[92] and the pore size and porosity cannot be controlled independently. In addition, so far this method has been applied only to a few synthetic hydrophilic polymers and some natural polymers for hydrogel applications.[91,93] The current successful pore formation in hydrogels through the gas injection method is mainly done on swollen cured hydrogels (i.e., in a batch process). To use this method in a continuous process similar to that used for polyolefin foams, more fundamental studies on simultaneous cross-linking and pressurizing/depressurizing should be done to define the phase diagram.

Phase Separation. Polymer solutions and blends will undergo phase separation if the free energy of mixing is positive. Phase separation continues until the complete separation of mixtures into multiple phases, which are not pure components. For example, if a polymer solution undergoes phase separation, we will have a polymer-lean and a polymer-rich phase. There are three mechanisms for phase separation: nucleation and growth, spinodal decomposition, and viscoelastic phase separation.[94−96] Phase separation can be exploited to make porous polymers, mainly through changing the temperature or adding an extra component to induce immiscibility. The commercialized phase separation method to produce porous polymers is non-solvent-induced phase separation (NIPS), which is widely used to produce membranes for water treatment.[97] Since hydrogels have a 3D molecular network, inducing porosity through phase separation can be rather complicated. The following approaches can be envisioned:

- nonsolvent dewatering of the as-synthesized hydrogels, in which an organic solvent (e.g., methanol or acetone) is used to remove the water from a swollen hydrogel leaving residual pores;[98]
- polymerization-induced phase separation, where the cross-linking and increases in molecular weight trigger the immiscibility of polymer in the water phase (in this process, microgels of the polymerizing phase can form and separate through aggregation);[99]
- cross-linking of phase-separating polymer solutions (e.g., the NIPS process on biopolymer solutions followed by cross-linking with diamine); and
- selective removal of a sacrificial phase in phase-separated polymer blends or block copolymers.[100,101]

It should be noted that the latter can also be classified as a templating method. Most of these methods have not been widely applied to produce porous hydrogels because they are not

https://doi.org/10.1021/acs.langmuir.2c02253
Langmuir XXXX, XXX, XXX−XXX

efficient for large-scale production. In fact, there are debates on the phase diagram of water-soluble polymers, especially biopolymers, due to the presence of hydrogen bonding and electrolytes,[102,103] which should be further studied to mature this method. Additionally, there is a need to evaluate how the porosity, pore size, and pore interconnectivity can be controlled by phase-separation methods.

Electrospinning. High electrical potentials can be used to draw charged threads with a submicrometer size from a polymer solution or melt. The electrical potential is applied between the spinning nozzle and a collector. During the spinning process, the fiber solidifies (through losing solvent, crystallization, gelation, etc.). The collected fibers, in the nanometer to micrometer range, are loosely connected and form a 3D mat that is porous. Electrospinning can be used to fabricate porous hydrogels, which are in the form of a mat of hydrogel fibers. The fiber diameter, porosity, and morphology of the porous mat are dependent on the solution variables (viscosity, solvent properties, electrical conductivity, and surface tension) and environmental conditions (temperature, humidity, and air velocity) but can be controlled by processing conditions (orifice size and shape, electrical potential, and the distance between the tip and the collector).[104,105]

Cross-linking is a critical step in the fabrication of porous hydrogels through electrospinning. Since the spinning process requires a sol/melt state for pumping through the nozzle and drawing toward the collector, the cross-linking step should be done postspinning or simultaneously. Apparently, the latter is more challenging since the molecular network formation should start after the ejection of sol/melt from the nozzle. Both physical and chemical cross-linking can be induced by exposure to bond-forming reagents, elevated temperature, and/or irradiation. There are reports in the literature on electrospun porous hydrogels from synthetic polymers, such as poly(acrylic acid)/poly(vinyl alcohol),[106] and natural polymers, such as gelatin and hyaluronic acid.[107,108] However, electrospinning has limitations in making 3D shapes (i.e., mainly planar shapes with limited thickness can be produced). Also, the mechanisms to control the porosity and pore size are the least developed compared to other techniques. The range of operational conditions to achieve uniform fibers is very narrow in many formulations. Addressing these three shortcomings can push electrospinning to become more viable for the large-scale production of porous hydrogels.

Freeze-Drying. If the solvent (usually water) in a synthesized hydrogel is crystallized and removed through sublimation (under high vacuum), then an interconnected macroporous structure will form. There is no limitation of the type of hydrogel that can be used in this technique, and the only requirement is the sublimation of the frozen solvent.[109] There have been reports on controlling the porous structure of freeze-dried hydrogels. For example, glutaraldehyde-cross-linked collagen−chitosan hydrogels have an open disordered pore structure when freeze-dried at −20 and −80 °C but show long planar-shaped pores when freeze-dried at −196 °C.[110] In other words, since the solvent crystals act as porogens, the shape and size of the pores replicate the formed crystals. However, we do not classify this method as a templating technique since the hydrogel 3D molecular network is formed prior to freeze-drying. In addition to the growth kinetics of solvent crystals, the nucleation of solvent strongly influences the porous structure. Morphological studies on the evolution of structure show that each pore is several orders of magnitude greater than the mesh size of the cross-linked network and is formed from the growth of one to a few ice grains.[111]

Heat transfer can also be exploited to direct the porous structure. For example, porous hydrogels with uniaxial linear pores are created by exposing only one side of the hydrogel to cooling (e.g., contacting with dry ice), inducing a uniaxial thermal gradient.[112] The current challenges with freeze-drying methods for the fabrication of porous hydrogels are as follows: lack of control over the pore size, weak mechanical properties, poor structural integrity, and collapse of pore structure if the material undergoes repeated swelling/deswelling cycles. On the fundamental side, to predict and design the porous structure via freeze-drying, future work can be done to better understand the thermodynamics and kinetics of water crystallization in hydrogel networks under isothermal and nonisothermal conditions.

Solid-Phase Templating. Solid particles can be employed as a template in forming pores within hydrogels. In this method, solid particles are often referred to as porogens and are typically added to the hydrogel precursor prior to cross-linking. The particles used are typically water-soluble, so they must reside in either the polymer phase or an organic solvent to prevent dissolution (e.g., the hydrogel polymer network is formed in an organic solvent containing NaCl particles). Once the hydrogel is cross-linked, the porogen is removed via leaching (e.g., through a water-washing step that dissolves the porogen and leaves a pore space). There are many water-soluble porogens that have been employed such as salt,[113−115] sugar,[116] and water-soluble polymer particles.[117,118]

Through this method, hydrogels can reach 40−74% porosity depending on the porogen and with the pore size ranging widely between 10 and 700 μm in diameter due to the various sizes of porogens.[119] Since this is a templating method, the resulting size of the pore is primarily determined by the size of the porogen. One of the most common porogen materials used is NaCl due to its abundance, grain-size range, and solubility. Particles of hydrophilic water-soluble polymers have also been used as porogens since their size can be tuned, for example when they are formed into beads through the precipitation of preformed polymers in (nano)droplets.[120] These beads can then be added to polymer solutions during cross-linking and leached out via water washing. For example, gelatin microbeads have been incorporated in poly(ethylene glycol)-diacrylate (PEGDA) that is cross-linked in an organic solvent. Then, the gelatin microbeads are removed by water washing, resulting in pore sizes ranging between 125 and 250 μm and materials with up to 60% porosity.[118] Cross-linked hydrophilic polymers can also be formed into beads and added as a solid-particle template wherein the cross-link bonds would then be disrupted in the leaching process.

The advantages of solid-particle templating methods are that they are economical in terms of both energy and material, do not require specialized equipment, and do not require the use of surfactants to stabilize the system. However, there could be difficulties in controlling the porosity as the porogen needs to be dispersed and distributed evenly into the hydrogel precursor. Also, this method does not guarantee an open-cell morphology. To increase the likelihood of interconnectivity, the volume fraction of salt to polymer needs to be >50 vol %.[121] The effectiveness of the porogen leaching is also a concern because it would be difficult to remove trapped porogen material when closed cell morphology is a possibility.[122] Organic solvent-based fabrication is common for this method to incorporate hydrophilic porogens but has environmental issues for large-scale

https://doi.org/10.1021/acs.langmuir.2c02253
Langmuir XXXX, XXX, XXX−XXX

manufacturing and cytotoxicity concerns for biomedical applications. The time required to leach out the porogens and dry the hydrogels is also another issue for large-scale fabrication.

To overcome some of these concerns, other methods have been used in tandem with particle leaching (e.g., gas generation[123] and freeze-drying[124]). Having two concurrent pore-generation methods can increase porosity and enhance interconnectivity. This also reduces the amount of porogen required to create porous hydrogels, making the leaching process more feasible. One main criterion for these dual pore-generation methods is that the porogen cannot be soluble in the solvent containing the polymer system.

An alternative to using solid particle additives as a porogen is the use of solvent crystals. This method, also known as freeze thawing and cryogelation, involves cooling the reaction mixture to form solvent crystals. Then, the polymerization step is performed. Finally, the interconnected porous structure is formed upon elimination of the solvent crystals.[109] This method should not be confused with freeze-drying in which the frozen crystals in the preformed hydrogel are removed through sublimation. Also, cryogelation involves solvent crystallization and is different from the sol−gel transition that takes place with decreasing temperature as, for example, in agarose or gelatin solutions. The interconnectivity of cryogels is due to the continuous fractal structure of solvent crystals.[109] While freeze-dried porous hydrogels are rigid and brittle, freeze−thawed porous hydrogels are soft and more elastic.[125] The structure and properties of cryogels are dependent on the composition and concentration of precursor, cross-linking type and reaction kinetics, cryogelation temperature, polymer molecular weight, water/organic cosolvent ratio, pH and ionic strength of the precursor, and cooling rate.[109,126] Additionally, the pore size control in cryogels should be investigated by using nucleating agents and the manipulation of crystallization kinetics by additives. The long list of parameters that influence the structure may suggest that controlling the pore size and porosity of cryogels is not as straightforward as the porous hydrogels fabricated via external solid-particle porogens.

Self-Assembled Amphiphile Templating. Surfactants self-assemble above a critical concentration to form micelles. Typically, at sufficiently high concentrations, lyotropic liquid-crystal (LLC) phases are obtained from the arrangement of micelles. LLCs are thermodynamically stable ordered structures that occur in mixtures of surfactants with one or several solvents. Depending on the shape of surfactants and the interfacial curvature, LLCs have different mesomorphic structures, such as lamellar, hexagonal, gyroid, and face-centered cubic.[127] Another class of thermodynamically stable systems is microemulsions, which are isotropic dispersions of oil and water stabilized by a surfactant system that provides ultralow surface tension. Microemulsions have nanometer-sized droplets or bicontinuous domains, described by Winsor classification. In phase diagrams of surfactant and selective solvent mixtures, LLC phases and microemulsion regions always seem disconnected.[128] While LLCs are highly ordered soft-condensed assemblies with specific nanometer-scale geometries, microemulsions have disordered structure.

Porous hydrogels have been synthesized from LLCs[127,129] and microemulsion[130] templates. Two common approaches are synergistic and transcriptive templating methods. In synergistic templating, polymerizable surfactants are used, in which the obtained material is the cross-linked template.[131] This method is not cost-effective and requires a new surfactant if a change in chemistry or domain size is desired. If monomers are used in the oil or water phase, then the templating process is called transcriptive, which results in a copy of the self-assembled structure.[131] Since commercially available monomers and surfactants can be used in this method, it is relatively more viable economically. There is a possibility that the template structure is not retained during polymerization (especially in transcriptive templating), but the self-assembled structure can still direct the polymer growth. Consequently, hierarchical morphologies can be formed, and such indirect templating is called reconstructive synthesis.[131,132]

Templating within LLCs and microemulsions is a complex process. The polymerization reaction progresses within a highly dynamic self-organized medium in a continuously changing physicochemical environment. In addition, since domains are in the nanometer range, a confinement effect is induced upon polymerization.[133] Many monomers show some degree of surface activity and consequently segregate at the interfaces.[131] Consequently, the polymerization can cause phase transitions by driving changes in the interface curvature. More severe effects may arise due to the loss of entropy or chemical incompatibility of the polymer with the surfactant, which sometimes drives phase separation and the concomitant disruption of the initial structure.[131] Retaining the nanosized domains in the microemulsion templates is an ongoing challenge, as only a limited number of studies show nanometer-sized porous hydrogels.[130] In contrast, more reports can be found on nanoporous hydrogels from LLC templating.[127] This observation can be attributed to the very low viscosity of microemulsions, which minimizes the kinetic stability against phase separation during polymerization, as well as their sensitivity to any increase in the interfacial tension between water and oil phases. While the templates of self-assembled amphiphiles, especially LLCs, provide unique control over the pore structure, pore size, and porosity, predictive tools for determining their phase diagram and domain size are still underdeveloped. In other words, most of the studies realize the domain size after the successful templating. Finally, a future direction is to perform systematic studies on the properties of ordered nanoporous hydrogels with the same composition but different mesomorphic structures to determine the constant for a second-order kinetic model and to validate models for structure-stiffness relationships and solute diffusion in porous hydrogels.

Emulsion Templating. Emulsions are kinetically stable dispersion of two or more immiscible liquids, which are stabilized by using surfactants or particles in the case of Pickering emulsions. High internal phase emulsions (HIPEs) are usually defined as emulsions in which the droplets are jammed and have a polyhedral shape (usually volume fraction $\phi > 0.74$). If the continuous phase of the HIPE is polymerized and the dispersed phase is removed, then porous polymers known as polyHIPEs are obtained.[134] Therefore, this method is known as emulsion templating or HIPE templating.

PolyHIPEs have an interconnected porous structure in which pores (also called voids) are replicas of emulsion droplets. Also, interconnecting holes, known as pore throats (or windows), usually exist between neighboring pores. The pore throats are formed due to the depletion-induced partial coalescence during polymerization and are influenced by the interdroplet interaction, drainage of the interdroplet layer, and interfacial rheology of the surfactant layer.[78,135] PolyHIPEs typically have pore sizes in the range of 1 to 30 μm and a pore throat size on the order of 0.5 to 3 μm. However, there are also reports on closed-

https://doi.org/10.1021/acs.langmuir.2c02253
Langmuir XXXX, XXX, XXX−XXX

pore polyHIPEs (e.g., in poly-Pickering-HIPEs).[78,136] Open-cell porous polymers have also been made with medium internal phase emulsion (MIPE) templates.[137] However, if the volume fraction is below 60%, achieving an interconnected porous structure is hardly possible. To make porous hydrogels, usually an oil-in-water emulsion is used, although hydrophilic porous polymers for hydrogel applications can also be produced from water-in-oil emulsions with careful selection of the two phases and the surfactant.[138]

One challenge with emulsion templating is to produce interconnected porous structures when the volume fraction of the dispersed phase is below 60%. Also, there are two areas for further development in emulsion templating: broadening the pore size range below 1 μm and beyond 30 μm and better control over the pore-throat size. To address the former, nanoemulsion templating should be considered to produce porous hydrogels with submicrometer pore size.[50] The pore size can be increased either by the polymerization of coarsening emulsions[138] or the development of new emulsifier systems. Alternatively, a foam templating method can be used,[54] which will be discussed in the next section. There are limited studies on controlling the pore-throat size. Successful approaches have reported the use of surfactant mixtures[135] and particle−surfactant mixtures.[139,140] However, fundamental studies should be done to correlate the pore-throat size with interdroplet interaction and interfacial rheology.

Foam Templating. Foam templating methods vary by degree of complexity. The simplest method of creating a foam template is through simple mechanical mixing or frothing. As the aqueous precursor solution is mixed rapidly, air is entrapped in the liquid. The foam then undergoes cross-linking to solidify the foam structure.[141−147] This produces a polydisperse porous structure that typically can reach high porosity of up to 80% and vary in pore size between 150 and 500 μm in diameter.[4] Interconnections between pores form with the same mechanism as described in the emulsion templating method (i.e., depletion induced partial coalescence during polymerization). The oldest report on making porous polymers via mechanical mixing was performed on air-whipped latex.[148]

For monodisperse foam templates, microfluidics devices are used to create uniform open-cell foams. Microfluidics inject gas bubbles individually in an extremely controlled system.[149−155] The major drawback to microfluidic systems is their limited scalability associated with their low production rate.[88] Foam templating can be incorporated into other templating methods such as emulsions termed "foamulsions".[156−159] This is where the gas is injected into the emulsion during mixing and trapped due to the emulsion's high viscosity. This results in two sources of porosity from the dispersed phase in the emulsion and the gas phase in the foam. This method also requires specialized equipment to inject gas into the emulsion since mechanically mixing the emulsion at high speeds for frothing can result in phase separation. The focus for the rest of this section will be on simple mechanical foaming.

Due to high interfacial tension and the difference in density of gases and liquids, foam templates are inherently unstable. The two main factors in foam stability for this method are viscosity[148] and interfacial tension.[54] The former, which is controlled by various factors (e.g., polymer structure, water content, and addition of thickening agents), can influence the rate of foam aging by changing the rate of gas diffusion through the liquid phase as well as coalescence. The liquid−air interfacial tension can be influenced by using stabilizers such as surfactants or particles that help reduce interfacial tension and are typically the cause of foaming for low-viscosity solutions. The rate of cross-linking is a major consideration due to the inherent instability of foam templates.

Synthetic porous polymers are typically difficult to make using this type of mechanical foaming due to their rather slow nature of cross-linking. Common methods of initiating polymerization include thermal, photo, and redox initiation. Unfortunately, increasing the temperature of the foam template impacts its stability, and UV light cannot effectively penetrate an opaque foam system. However, redox initiation is one possible method since it can occur rapidly at room temperature. The other main concern with synthetic polymers is the oxygen inhibition of free-radical polymerization, which means that air cannot be used as a dispersed gas phase. This requires either an enclosed inert gas atmosphere during the mechanical mixing or closed systems where the gas is added such as in an interconnected syringe method.[54]

Biopolymers are typically sought for this type of mechanical foaming for two reasons. First, they are typically water-thickening agents, thus their solution viscosity is high. Second, they have rapid cross-linking by either a covalent or ionic mechanism. For example, chitosan can be rapidly covalently cross-linked using an agent such as glutaraldehyde[160] or genipin,[161] while alginate can be ionically cross-linked instantaneously by a multivalent cation such as calcium (Ca^{2+}) or iron (Fe^{3+}).[162]

The main advantage to using a foam templating method is that the sacrificial template is a low-cost gas phase and processing typically requires only basic equipment. The porosity and pore morphology can be tuned through process parameters such as mixing geometry (e.g., whisk and blade), longer mixing times, and higher mixing speeds to trap more of the gas phase and increase the pore size uniformity (similar to that of emulsion templates). The volume fraction of the gas phase in the foam system can also be controlled via either the amount of gas injected or the amount of mixing to reach a desired change in volume of the foam template. The main disadvantage to using this method is the foam instability, making the control of pore size and porosity challenging. To trap the desired pore size and porosity, the cross-linking mechanism needs to be rapid enough to prevent foam coalescence or collapse. There is also typically a lack of pore interconnectivity for this method due to the higher interfacial tension of the liquid−gas system. In addition, foam templating is less developed than other methods, but it is material-efficient, does not need porogens to form the porous structure, and needs less energy than the gas injection method. However, better mixing and frothing methods should be developed to enable large-scale production.

CONCLUDING REMARKS

In this feature article, we described the classification of porous hydrogels and distinguished between the spaces within the polymer network itself and the imbedded pores. Two mechanisms control the performance of porous hydrogels: diffusion and capillary action. We defined porous hydrogels as hydrogels in which the latter is not negligible. We proposed new routes to model the physical properties of porous hydrogels by elaborating on current theories for dense hydrogels with respect to swelling kinetics, equilibrium swelling capacity, structure−stiffness relationships, and solute diffusion. The reviewed models were compared with experimentally measured swelling kinetics of dense and nondense hydrogels, which clearly showed

https://doi.org/10.1021/acs.langmuir.2c02253
Langmuir XXXX, XXX, XXX−XXX

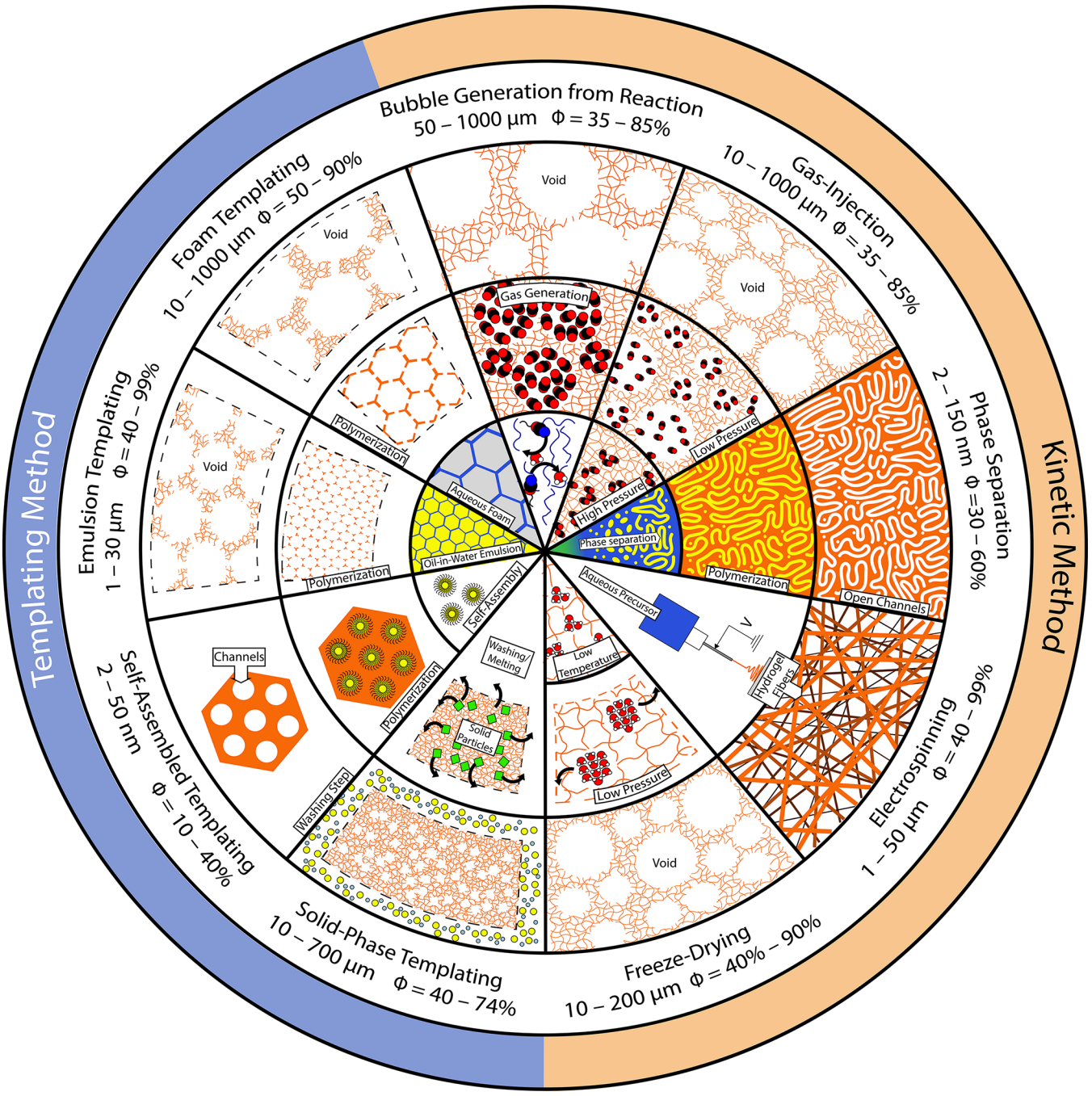

Figure 4. Summary of methods for producing porous hydrogels. Moving from the center outward, the production stages are schematically shown. In addition, the common pore size and porosity ranges for each method are also included.

that except for the second-order kinetics model, none of them deliver a satisfactory prediction. Since further development of these models requires more experimental studies on hydrogels with different porous structure, we described methods for making porous hydrogels. In this regard, the basics of kinetic and templating methods and their governing parameters were discussed as schematically shown in Figure 4. Then, the limitations of each method and potential future work were elaborated, as summarized in Table 3.

Considering that there is a wide variation in pore size and porosity in each of the listed methods, it is impossible to specify how physical properties will be different among these methods (as can be seen in Figure 2 as an example) and their comparison will need detailed systematic studies. We believe that the templating methods can produce porous hydrogels with controlled pore size, shape, and interconnectivity. Therefore, systematic studies can be performed on the physical properties of such hydrogels to improve current models, which may lead to new understanding. Beyond what is discussed in the different sections, environmental concerns should be considered for making porous hydrogels. For example, the fabrication method should have minimum waste, production energy, and need for recovery of byproducts and the template (note that in this sense, foam templating has the greatest potential). In addition, it is preferred to have biobased monomers or precursors for hydrogel synthesis and to produce biodegradable porous hydrogels with

https://doi.org/10.1021/acs.langmuir.2c02253
Langmuir XXXX, XXX, XXX−XXX

Table 3. Comparison of Methods for Making Porous Hydrogels

Method	Challenges	Opportunities
bubble generation from reaction	• limited solubility of many chemical blowing agents in aqueous media • water loss due to evaporation for thermally activated blowing agents • difficulty in controlling and reproducing the pore size and porosity • high gas solubility can suppress foaming or destabilize the foaming in the bubble generation from reaction	• effect of elongational rheology of the continuous phase and the interfacial rheology on bubble growth • using surfactants and nanoparticles to control the pore size and porosity
gas injection in polymer melt or precursor	• high gas solubility can suppress foaming or destabilize the foaming in the bubble generation from reaction • noneconomical foaming of hydrogels with sc-CO_2	• effect of elongational rheology of the continuous phase and the interfacial rheology on bubble growth • simultaneous cross-linking and pressurizing/depressurizing for continuous processing
phase separation	• controversy in the phase diagram of water-soluble polymers due to the presence of hydrogen bonding and electrolytes • controlling porosity, pore size, and pore interconnectivity	• determining the phase diagram of water-soluble polymers and polymerizing systems in the presence of water and nonsolvent
electrospinning	• preforming cross-linking simultaneously or as a postspinning step • limitations in making 3D shapes • least-developed methodologies for controlling the porosity and pore size	• co-spinning of hydrogels with different chemistries for synergistic properties • multilayer hydrogel mats
freeze-drying	• controlling porosity, pore size, and pore interconnectivity • poor structural integrity and mechanical properties • structural collapse upon undergoing repeated swelling/deswelling cycles	• directing the porous structure by controlling heat transfer • determining thermodynamics and kinetics of crystallization of water in hydrogel networks
solid-phase templating	• even dispersion and distribution of porogen into the hydrogel precursor • no guarantee of resulting in an open-cell morphology • time for leaching out the porogen and the cost of recovering it	• candidate for dual-pore-generation formulations
self-assembled amphiphiles templating	• can be costly if synergistic templating is used • retaining the nanosized domains • underdeveloped predictive tools for determining domain size	• making isoporous hydrogels for fundamental studies and high-end applications
emulsion templating	• producing interconnected porous structures when the volume fraction of the dispersed phase is <60% • templating pore size below 1 μm and beyond 30 μm • limitations on controlling the pore-throat size	• nanoemulsion-templated porous polymers • 3D printing
foam templating	• producing interconnected porous structures when the volume fraction of the dispersed phase is <60% • noticeable instability of foam templates	• implementation of covalent or ionic co-crosslinking or double network • enhanced mixing methods for large-scale production

minimal side effects on living species. Another consideration is to use green solvents, such as ionic liquids, if the process cannot be carried out in a solvent-free approach.

AUTHOR INFORMATION

Corresponding Author

Donald L. Feke − *Department of Chemical and Biomolecular Engineering, Case Western Reserve University, Cleveland, Ohio 44106, United States;* orcid.org/0000-0003-4707-4050; Email: donald.feke@case.edu

Authors

Reza Foudazi − *School of Chemical, Biological, and Materials Engineering, University of Oklahoma, Norman, Oklahoma 73069, United States;* orcid.org/0000-0001-6711-3390

Ryan Zowada − *Department of Chemical and Materials Engineering, New Mexico State University, Las Cruces, New Mexico 88003, United States*

Ica Manas-Zloczower − *Department of Macromolecular Science & Engineering, Case Western Reserve University, Cleveland, Ohio 44106, United States;* orcid.org/0000-0001-7522-1930

Complete contact information is available at: https://pubs.acs.org/10.1021/acs.langmuir.2c02253

Notes

The authors declare no competing financial interest.

Biographies

Reza Foudazi is an associate professor in the School of Chemical, Biological, and Materials Engineering at the University of Oklahoma.

https://doi.org/10.1021/acs.langmuir.2c02253
Langmuir XXXX, XXX, XXX−XXX

Before joining the University of Oklahoma in 2021, he was a tenured associate professor at New Mexico State University. He received his B.S. and M.S. in polymer engineering from Amirkabir University of Technology (Tehran, Iran) and his doctorate from Cape Peninsula University of Technology (Cape Town, South Africa). The current research activities in his group are the self-assembly of amphiphilic molecules, templating approach for the synthesis of porous polymers, and rheology of soft matter, with the long-term goal of producing responsive multifunctional materials for sustainability and environmental applications.

Ryan Zowada received his B.S. degree in chemical engineering at New Mexico State University in 2016. He later received his Ph.D. in chemical engineering with Prof. Reza Foudazi at New Mexico State University in 2021. He is currently holding a postdoctoral position in the College of Engineering at New Mexico State University. His scientific interests involve the development of porous polymers for wide-ranging applications involving environmental remediation, medical devices, and water treatment.

Ica Manas-Zloczower is the Thomas W. and Nancy P. Seitz Professor of Advanced Materials and Energy in the Department of Macromolecular Science and Engineering and the Distinguished University Professor at Case Western Reserve University. She received her B.S. and M.S. degrees in chemical engineering from Polytechnic Institute Jassy, Romania and a Doctor of Science in chemical engineering from the Technion-Israel Institute of Technology. She was a postdoctoral fellow at the University of Minnesota. Professor Manas-Zloczower's current research interests include engineering new materials and technologies for industrial applications, including high internal phase emulsion templating technologies for open-pore-structure materials.

Donald L. Feke earned his B.S. and M.S. degrees from Case Western Reserve University (1976 and 1977) and a Ph.D. from Princeton University (1981), all in chemical engineering. He joined the faculty at Case Western Reserve University in 1981 and has been pursuing dual faculty−administrative roles since 1997. Research interests include the physical behavior and processing characteristics of multiphase (particle−liquid or fluid−liquid) dispersions. He has also developed several methods that use resonant ultrasonic fields to perform sharp separations with applications in chemical and biochemical processing

REFERENCES

(1) Enomoto-Rogers, Y.; Kimura, S.; Iwata, T. Soft, Tough, and Flexible Curdlan Hydrogels and Organogels Fabricated by Covalent Cross-Linking. *Polymer (Guildf)* **2016**, *100*, 143−148.

(2) Mahdavinia, G. R.; Pourjavadi, A.; Hosseinzadeh, H.; Zohuriaan, M. J. Superabsorbent Hydrogels from Poly(Acrylic Acid-Co Acrylamide) Grafted Chitosan with Salt and PH-Reponsiveness Properties. *Eur. Polym. J.* **2004**, *40*, 1399−1407.

(3) Hart, L. F.; Hertzog, J. E.; Rauscher, P. M.; Rawe, B. W.; Tranquilli, M. M.; Rowan, S. J. Material Properties and Applications of Mechanically Interlocked Polymers. *Nat. Rev. Mater.* **2021**, *6* (6), 508−530.

(4) Djemaa, I.; Ben; Auguste, S.; Drenckhan-Andreatta, W.; Andrieux, S. Hydrogel Foams from Liquid Foam Templates: Properties and Optimisation. *Adv. Colloid Interface Sci.* **2021**, *294* (June), 102478.

(5) Ahmed, E. M. Hydrogel: Preparation, Characterization, and Applications: A Review. *J. Adv. Res.* **2015**, *6* (2), 105−121.

(6) Zhang, Y. S.; Khademhosseini, A. Advances in Engineering Hydrogels. *Science* **2017**, *356* (6337), eaaf3627.

(7) Wilker, J. J. Sticky When Wet. *Nat. Mater.* **2014**, *13* (9), 849−850.

(8) Peak, C. W.; Wilker, J. J.; Schmidt, G. A Review on Tough and Sticky Hydrogels. *Colloid Polym. Sci.* **2013**, *291* (9), 2031−2047.

(9) Taylor, D. L.; in het Panhuis, M. Self-healing Hydrogels. *Adv. Mater.* **2016**, *28* (41), 9060−9093.

(10) Gaharwar, A. K.; Dammu, S. A.; Canter, J. M.; Wu, C.-J.; Schmidt, G. Highly Extensible, Tough, and Elastomeric Nanocomposite Hydrogels from Poly (Ethylene Glycol) and Hydroxyapatite Nanoparticles. *Biomacromolecules* **2011**, *12* (5), 1641−1650.

(11) Ganji, F.; Vasheghani-Farahani, S.; Vasheghani-Farahani, E. Theoretical Description of Hydrogel Swelling: A Review. *Iran. Polym. J.* **2010**, *19* (5), 375−398.

(12) Chen, J.; Park, H.; Park, K. Synthesis of Superporous Hydrogels: Hydrogels with Fast Swelling and Superabsorbent Properties. *J. Biomed. Mater. Res.* **1999**, *44* (1), 53−62.

(13) Zdravkov, B.; Čermák, J.; Šefara, M.; Janků, J. Pore Classification in the Characterization of Porous Materials: A Perspective. *Open Chem.* **2007**, *5* (2), 385−395.

(14) Amsden, B. G. Hydrogel Mesh Size and Its Impact on Predictions of Mathematical Models of the Solute Diffusion Coefficient. *Macromolecules* **2022**, *55* (18), 8399−8408.

(15) Lee-Wang, H. H.; Blakey, I.; Chirila, T. V.; Peng, H.; Rasoul, F.; Whittaker, A. K.; Dargaville, B. L. Novel Supramolecular Hydrogels as Artificial Vitreous Substitutes. *Macromol. Symp.* **2010**, *296* (Modern Trends in PolymerScience–EPF'09), 229−232.

(16) Nair, L. S.; Laurencin, C. T.; Tandon, M.*Injectable Hydrogels as Biomaterials*; John Wiley & Sons: Hoboken, NJ, 2010.

(17) Liu, Z.; Calvert, P. Multilayer Hydrogels as Muscle-like Actuators. *Adv. Mater.* **2000**, *12* (4), 288−291.

(18) Emami, Z.; Ehsani, M.; Zandi, M.; Daemi, H.; Ghanian, M.-H.; Foudazi, R. Modified Hydroxyapatite Nanoparticles Reinforced Nanocomposite Hydrogels Based on Gelatin/Oxidized Alginate via Schiff Base Reaction. *Carbohydr. Polym. Technol. Appl.* **2021**, *2*, 100056.

(19) Lin, C.-C.; Metters, A. T. Hydrogels in Controlled Release Formulations: Network Design and Mathematical Modeling. *Adv. Drug Delivery Rev.* **2006**, *58* (12−13), 1379−1408.

(20) Gupta, P.; Vermani, K.; Garg, S. Hydrogels: From Controlled Release to PH-Responsive Drug Delivery. *Drug Discovery Today* **2002**, *7* (10), 569−579.

(21) Sharpe, L. A.; Daily, A. M.; Horava, S. D.; Peppas, N. A. Therapeutic Applications of Hydrogels in Oral Drug Delivery. *Expert Opin. Drug Delivery* **2014**, *11* (6), 901−915.

(22) Zhang, S.; Fan, X.; Zhang, F.; Zhu, Y.; Chen, J. Synthesis of Emulsion-Templated Magnetic Porous Hydrogel Beads and Their Application for Catalyst of Fenton Reaction. *Langmuir* **2018**, *34* (12), 3669−3677.

(23) Bahsis, L.; Ablouh, E.-H.; Anane, H.; Taourirte, M.; Julve, M.; Stiriba, S.-E. Cu (II)-Alginate-Based Superporous Hydrogel Catalyst for Click Chemistry Azide−Alkyne Cycloaddition Type Reactions in Water. *RSC Adv.* **2020**, *10* (54), 32821−32832.

(24) Sun, X.; Yao, F.; Li, J. Nanocomposite Hydrogel-Based Strain and Pressure Sensors: A Review. *J. Mater. Chem. A* **2020**, *8* (36), 18605−18623.

(25) Yetisen, A. K.; Butt, H.; Volpatti, L. R.; Pavlichenko, I.; Humar, M.; Kwok, S. J. J.; Koo, H.; Kim, K. S.; Naydenova, I.; Khademhosseini, A. Photonic Hydrogel Sensors. *Biotechnol. Adv.* **2016**, *34* (3), 250−271.

(26) Zowada, R.; Foudazi, R. Porous Hydrogels Embedded with Hydrated Ferric Oxide Nanoparticles for Arsenate Removal. *ACS Appl. Polym. Mater.* **2019**, *1* (5), 1006−1014.

(27) Abbasian Chaleshtari, Z.; Foudazi, R. Polypyrrole@polyHIPE Composites for Hexavalent Chromium Removal from Water. *ACS Appl. Polym. Mater.* **2020**, *2* (8), 3196−3204.

(28) Getachew, B. A.; Kim, S.-R.; Kim, J.-H. Self-Healing Hydrogel Pore-Filled Water Filtration Membranes. *Environ. Sci. Technol.* **2017**, *51* (2), 905−913.

(29) Jie, G.; Kongyin, Z.; Xinxin, Z.; Zhijiang, C.; Min, C.; Tian, C.; Junfu, W. Preparation and Characterization of Carboxyl Multi-Walled Carbon Nanotubes/Calcium Alginate Composite Hydrogel Nanofiltration Membrane. *Mater. Lett.* **2015**, *157*, 112−115.

(30) Qin, D.; Liu, Z.; Liu, Z.; Bai, H.; Sun, D. D. Superior Antifouling Capability of Hydrogel Forward Osmosis Membrane for Treating Wastewaters with High Concentration of Organic Foulants. *Environ. Sci. Technol.* **2018**, *52* (3), 1421−1428.

https://doi.org/10.1021/acs.langmuir.2c02253
Langmuir XXXX, XXX, XXX−XXX

(31) Batista, R. A.; Espitia, P. J. P.; Quintans, J.; de, S. S.; Freitas, M. M.; Cerqueira, M. A.; Teixeira, J. A.; Cardoso, J. C. Hydrogel as an Alternative Structure for Food Packaging Systems. *Carbohydr. Polym.* **2019**, *205*, 106−116.
(32) Shewan, H. M.; Stokes, J. R. Review of Techniques to Manufacture Micro-Hydrogel Particles for the Food Industry and Their Applications. *J. Food Eng.* **2013**, *119* (4), 781−792.
(33) Qu, B.; Luo, Y. Chitosan-Based Hydrogel Beads: Preparations, Modifications and Applications in Food and Agriculture Sectors−A Review. *Int. J. Biol. Macromol.* **2020**, *152*, 437−448.
(34) Rudzinski, W. E.; Dave, A. M.; Vaishnav, U. H.; Kumbar, S. G.; Kulkarni, A. R.; Aminabhavi, T. M. Hydrogels as Controlled Release Devices in Agriculture. *Des. monomers Polym.* **2002**, *5* (1), 39−65.
(35) Cheng, D.; Liu, Y.; Yang, G.; Zhang, A. Water-and Fertilizer-Integrated Hydrogel Derived from the Polymerization of Acrylic Acid and Urea as a Slow-Release N Fertilizer and Water Retention in Agriculture. *J. Agric. Food Chem.* **2018**, *66* (23), 5762−5769.
(36) El-Rehim, H. A. A.; Hegazy, E. A.; El-Mohdy, H. L. A. Radiation Synthesis of Hydrogels to Enhance Sandy Soils Water Retention and Increase Plant Performance. *J. Appl. Polym. Sci.* **2004**, *93* (3), 1360−1371.
(37) Wade, E.; Zowada, R.; Foudazi, R. Alginate and Guar Gum Spray Application for Improving Soil Aggregation and Soil Crust Integrity. *Carbohydr. Polym. Technol. Appl.* **2021**, *2*, 100114.
(38) Jensen, O. M.; Hansen, P. F. Water-Entrained Cement-Based Materials: II. Experimental Observations. *Cem. Concr. Res.* **2002**, *32* (6), 973−978.
(39) Hoffman, A. S. Hydrogels for Biomedical Applications. *Adv. Drug Delivery Rev.* **2012**, *64*, 18−23.
(40) Bajpai, A. K.; Shukla, S. K.; Bhanu, S.; Kankane, S. Responsive Polymers in Controlled Drug Delivery. *Prog. Polym. Sci.* **2008**, *33* (11), 1088−1118.
(41) Peppas, N. A.; Korsmeyer, R. W.Dynamically Swelling Hydrogels in Controlled Release Applications. In *Hydrogels in Medicine and Pharmacy*; Peppas, N. A., Ed.; CRC Press: Boca Raton, FL, 1987; Vol. 3, pp 109−136.
(42) Cai, W.; Gupta, R. B. Poly (N-Ethylacrylamide) Hydrogels for Lignin Separation. *Ind. Eng. Chem. Res.* **2001**, *40* (15), 3406−3412.
(43) Schott, H. Swelling Kinetics of Polymers. *J. Macromol. Sci. Part B* **1992**, *31* (1), 1−9.
(44) Andrews, D. H.; Johnston, J. The Rate of Absorption of Water by Rubber. *J. Am. Chem. Soc.* **1924**, *46* (3), 640−650.
(45) Quintana, J. R.; Valderruten, N. E.; Katime, I. Synthesis and Swelling Kinetics of Poly(Dimethylaminoethyl Acrylate Methyl Chloride Quaternary-Co-Itaconic Acid) Hydrogels. *Langmuir* **1999**, *15* (14), 4728−4730.
(46) Malakian, A.; Zhou, M.; Zowada, R. T.; Foudazi, R. Synthesis and in Situ Functionalization of Microfiltration Membranes via High Internal Phase Emulsion Templating. *Polym. Int.* **2019**, *68* (7), 1378−1386.
(47) Adnadjevic, B.; Jovanovic, J. Novel Approach in Investigation of the Poly (Acrylic Acid) Hydrogel Swelling Kinetics in Water. *J. Appl. Polym. Sci.* **2008**, *107* (6), 3579−3587.
(48) Omidian, H.; Hashemi, S. A.; Sammes, P. G.; Meldrum, I. A Model for the Swelling of Superabsorbent Polymers. *Polymer (Guildf)* **1998**, *39* (26), 6697−6704.
(49) Benmessaoud, N.; Hamri, S.; Bouchaour, T.; Maschke, U. Swelling and Thermal Behavior of a Cross-Linked Polymer Networks Poly(2-Phenoxyethyl Acrylate): Exploitation by the Voigt Viscoelastic Model. *Polym. Bull.* **2020**, *77* (10), 5567−5588.
(50) Abbasian Chaleshtari, Z.; Salimi-Kenari, H.; Foudazi, R. Interdroplet Interactions and Rheology of Concentrated Nanoemulsions for Templating Porous Polymers. *Langmuir* **2021**, *37* (1), 76−89.
(51) Zhmud, B. V.; Tiberg, F.; Hallstensson, K. Dynamics of Capillary Rise. *J. Colloid Interface Sci.* **2000**, *228* (2), 263−269.
(52) Hamraoui, A.; Nylander, T. Analytical Approach for the Lucas-Washburn Equation. *J. Colloid Interface Sci.* **2002**, *250* (2), 415−421.
(53) Hall, C.; Yau, M. H. R. Water Movement in Porous Building Materials—IX. The Water Absorption and Sorptivity of Concretes. *Build. Environ.* **1987**, *22* (1), 77−82.
(54) Zowada, R.; Foudazi, R. Polyfoam: Foam-Templated Microcellular Polymers. *Langmuir* **2020**, *36* (27), 7868−7878.
(55) Cohn, P. G.; Qavi, S.; Cubuk, J.; Jani, M.; Megdad, M. L.; Shah, D.; Cattafi, C.; Baul, P.; Rajaraman, S.; Foudazi, R. Getting Control of Hydrogel Networks with Cross-Linkable Monomers. *J. Mater. Chem. B* **2021**, *9* (46), 9497−9504.
(56) Peppas, N. A.; Merrill, E. W. Crosslinked Poly (Vinyl Alcohol) Hydrogels as Swollen Elastic Networks. *J. Appl. Polym. Sci.* **1977**, *21* (7), 1763−1770.
(57) Bray, J. C.; Merrill, E. W. Poly (Vinyl Alcohol) Hydrogels. Formation by Electron Beam Irradiation of Aqueous Solutions and Subsequent Crystallization. *J. Appl. Polym. Sci.* **1973**, *17* (12), 3779−3794.
(58) Flory, P. J.; Rehner, J. Statistical Mechanics of Cross-Linked Polymer Networks I. Rubberlike Elasticity. *J. Chem. Phys.* **1943**, *11* (11), 512−520.
(59) Flory, P. J.; Rehner, J. Statistical Mechanics of Cross-Linked Polymer Networks II. Swelling. *J. Chem. Phys.* **1943**, *11* (11), 521−526.
(60) McKenna, G. B.; Horkay, F. Effect of Crosslinks on the Thermodynamics of Poly(Vinyl Alcohol) Hydrogels. *Polymer (Guildf)* **1994**, *35* (26), 5737−5742.
(61) Richbourg, N. R.; Peppas, N. A. The Swollen Polymer Network Hypothesis: Quantitative Models of Hydrogel Swelling, Stiffness, and Solute Transport. *Prog. Polym. Sci.* **2020**, *105*, 101243.
(62) James, H. M.; Guth, E. Statistical Thermodynamics of Rubber Elasticity. *J. Chem. Phys.* **1953**, *21* (6), 1039−1049.
(63) Treloar, L. R. G.*The Physics of Rubber Elasticity*; OUP: Oxford, 1975.
(64) Oyen, M. L. Mechanical Characterisation of Hydrogel Materials. *Int. Mater. Rev.* **2014**, *59* (1), 44−59.
(65) Emami, Z.; Ehsani, M.; Zandi, M.; Foudazi, R. Controlling Alginate Oxidation Conditions for Making Alginate-Gelatin Hydrogels. *Carbohydr. Polym.* **2018**, *198*, 509−517.
(66) Biot, M. A. General Theory of Three-dimensional Consolidation. *J. Appl. Phys.* **1941**, *12* (2), 155−164.
(67) Lai, Y.; Hu, Y. Probing the Swelling-Dependent Mechanical and Transport Properties of Polyacrylamide Hydrogels through AFM-Based Dynamic Nanoindentation. *Soft Matter* **2018**, *14* (14), 2619−2627.
(68) Kalcioglu, Z. I.; Mahmoodian, R.; Hu, Y.; Suo, Z.; Van Vliet, K. J. From Macro-to Microscale Poroelastic Characterization of Polymeric Hydrogels via Indentation. *Soft Matter* **2012**, *8* (12), 3393−3398.
(69) Wang, Q.-M.; Mohan, A. C.; Oyen, M. L.; Zhao, X.-H. Separating Viscoelasticity and Poroelasticity of Gels with Different Length and Time Scales. *Acta Mech. Sin.* **2014**, *30* (1), 20−27.
(70) Wang, X.; Hong, W. A Visco-Poroelastic Theory for Polymeric Gels. *Proc. R. Soc. A Math. Phys. Eng. Sci.* **2012**, *468* (2148), 3824−3841.
(71) Zhan, Y.; Niu, X. Tuning Methods and Mechanical Modelling of Hydrogels. *Bioinspired, Biomim. Nanobiomaterials* **2015**, *4* (2), 140−154.
(72) Canal, T.; Peppas, N. A. Correlation between Mesh Size and Equilibrium Degree of Swelling of Polymeric Networks. *J. Biomed. Mater. Res.* **1989**, *23* (10), 1183−1193.
(73) Peppas, N. A.; Reinhart, C. T. Solute Diffusion in Swollen Membranes. Part I. A New Theory. *J. Membr. Sci.* **1983**, *15* (3), 275−287.
(74) Reinhart, C. T.; Peppas, N. A. Solute Diffusion in Swollen Membranes. Part II. Influence of Crosslinking on Diffusive Properties. *J. Membr. Sci.* **1984**, *18*, 227−239.
(75) Ogston, A. G.; Preston, B. N.; Wells, J. D. On the Transport of Compact Particles through Solutions of Chain-Polymers. *Proc. R. Soc. London. A. Math. Phys. Sci.* **1973**, *333* (1594), 297−316.
(76) Tartakovsky, D. M.; Dentz, M. Diffusion in Porous Media: Phenomena and Mechanisms. *Transp. Porous Media* **2019**, *130* (1), 105−127.

https://doi.org/10.1021/acs.langmuir.2c02253
Langmuir XXXX, XXX, XXX−XXX

(77) Cantat, I.; Cohen-Addad, S.; Elias, F.; Graner, F.; Höhler, R.; Pitois, O.; Rouyer, F.; Saint-Jalmes, A.; Flatman, R.; Cox, S.*Foams: Structure and Dynamics*.; Oxford University Press, 2013.
(78) Foudazi, R. HIPEs to PolyHIPEs. *React. Funct. Polym.* **2021**, *164*, 104917.
(79) Colton, J. S.; Suh, N. P. Nucleation of Microcellular Foam: Theory and Practice. *Polym. Eng. Sci.* **1987**, *27* (7), 500−503.
(80) Ramesh, N. S.Fundamentals of Bubble Nucleation and Growth in Polymers. In *Polymeric Foams*; CRC Press, 2004; pp 76−107.
(81) Goel, S. K.; Beckman, E. J. Nucleation and Growth in Microcellular Materials: Supercritical CO2 as Foaming Agent. *AIChE J.* **1995**, *41* (2), 357−367.
(82) Mihai, M.; Huneault, M. A.; Favis, B. D. Rheology and Extrusion Foaming of Chain-branched Poly (Lactic Acid). *Polym. Eng. Sci.* **2010**, *50* (3), 629−642.
(83) Ruengphrathuengsuka, W.*Bubble Nucleation and Growth Dynamics in Polymer Melts*. Ph.D. Dissertation; Texas A&M University, 1992.
(84) Lifshitz, I. M.; Slyozov, V. V. The Kinetics of Precipitation from Supersaturated Solid Solutions. *J. Phys. Chem. Solids* **1961**, *19* (1−2), 35−50.
(85) Zeeb, B.; Gibis, M.; Fischer, L.; Weiss, J. Influence of Interfacial Properties on Ostwald Ripening in Crosslinked Multilayered Oil-in-Water Emulsions. *J. Colloid Interface Sci.* **2012**, *387* (1), 65−73.
(86) Lundin, J. G.; Daniels, G. C.; McGann, C. L.; Stanbro, J.; Watters, C.; Stockelman, M.; Wynne, J. H. Multi-Functional Polyurethane Hydrogel Foams with Tunable Mechanical Properties for Wound Dressing Applications. *Macromol. Mater. Eng.* **2017**, *302* (3), 1600375.
(87) Coste, G.; Negrell, C.; Caillol, S. From Gas Release to Foam Synthesis, the Second Breath of Blowing Agents. *Eur. Polym. J.* **2020**, *140* (July), 110029.
(88) Andrieux, S.; Quell, A.; Stubenrauch, C.; Drenckhan, W. Liquid Foam Templating − A Route to Tailor-Made Polymer Foams. *Adv. Colloid Interface Sci.* **2018**, *256*, 276−290.
(89) Jones, S. F.; Evans, G. M.; Galvin, K. P. Bubble Nucleation from Gas Cavities — a Review. *Adv. Colloid Interface Sci.* **1999**, *80* (1), 27−50.
(90) Tsioptsias, C.; Paraskevopoulos, M. K.; Christofilos, D.; Andrieux, P.; Panayiotou, C. Polymeric Hydrogels and Supercritical Fluids: The Mechanism of Hydrogel Foaming. *Polymer (Guildf)* **2011**, *52* (13), 2819−2826.
(91) Dehghani, F.; Annabi, N. Engineering Porous Scaffolds Using Gas-Based Techniques. *Curr. Opin. Biotechnol.* **2011**, *22* (5), 661−666.
(92) Tsioptsias, C.; Stefopoulos, A.; Kokkinomalis, I.; Papadopoulou, L.; Panayiotou, C. Development of Micro-and Nano-Porous Composite Materials by Processing Cellulose with Ionic Liquids and Supercritical CO 2. *Green Chem.* **2008**, *10* (9), 965−971.
(93) Annabi, N.; Mithieux, S. M.; Boughton, E. A.; Ruys, A. J.; Weiss, A. S.; Dehghani, F. Synthesis of Highly Porous Crosslinked Elastin Hydrogels and Their Interaction with Fibroblasts in Vitro. *Biomaterials* **2009**, *30* (27), 4550−4557.
(94) Bates, F. S. Polymer-Polymer Phase Behavior. *Science (80-.)* **1991**, *251* (4996), 898−905.
(95) Khademzadeh Yeganeh, J.; Goharpey, F.; Foudazi, R. Rheology and Morphology of Dynamically Asymmetric LCST Blends: Polystyrene/Poly(Vinyl Methyl Ether. *Macromolecules* **2010**, *43* (20), 8670−8685.
(96) Yeganeh, J. K.; Goharpey, F.; Foudazi, R. Anomalous Phase Separation Behavior in Dynamically Asymmetric LCST Polymer Blends. *RSC Adv.* **2014**, *4* (25), 12809−12825.
(97) Lessan, F.; Foudazi, R. Effect of [EMIM][BF4] Ionic Liquid on the Properties of Ultrafiltration Membranes. *Polymer (Guildf)* **2020**, *210*, 122977.
(98) Kabiri, K.; Zohuriaan-Mehr, M. J. Porous Superabsorbent Hydrogel Composites: Synthesis, Morphology and Swelling Rate. *Macromol. Mater. Eng.* **2004**, *289* (7), 653−661.
(99) Okay, O. Macroporous Copolymer Networks. *Prog. Polym. Sci.* **2000**, *25* (6), 711−779.
(100) Seo, M.; Kim, S.; Oh, J.; Kim, S.-J.; Hillmyer, M. A. Hierarchically Porous Polymers from Hyper-Cross-Linked Block Polymer Precursors. *J. Am. Chem. Soc.* **2015**, *137* (2), 600−603.
(101) Saba, S. A.; Mousavi, M. P. S.; Bühlmann, P.; Hillmyer, M. A. Hierarchically Porous Polymer Monoliths by Combining Controlled Macro-and Microphase Separation. *J. Am. Chem. Soc.* **2015**, *137* (28), 8896−8899.
(102) Frith, W. J. Mixed Biopolymer Aqueous Solutions−Phase Behaviour and Rheology. *Adv. Colloid Interface Sci.* **2010**, *161* (1−2), 48−60.
(103) Halperin, A.; Kröger, M.; Winnik, F. M. Poly (N-isopropylacrylamide) Phase Diagrams: Fifty Years of Research. *Angew. Chemie Int. Ed.* **2015**, *54* (51), 15342−15367.
(104) Annabi, N.; Nichol, J. W.; Zhong, X.; Ji, C.; Koshy, S.; Khademhosseini, A.; Dehghani, F. Controlling the Porosity and Microarchitecture of Hydrogels for Tissue Engineering. *Tissue Eng. Part B Rev.* **2010**, *16* (4), 371−383.
(105) Ghosh, T.; Das, T.; Purwar, R. Review of Electrospun Hydrogel Nanofiber System: Synthesis, Properties and Applications. *Polym. Eng. Sci.* **2021**, *61* (7), 1887−1911.
(106) Li, L.; Hsieh, Y.-L. Ultra-Fine Polyelectrolyte Hydrogel Fibres from Poly (Acrylic Acid)/Poly (Vinyl Alcohol). *Nanotechnology* **2005**, *16* (12), 2852−2860.
(107) Panzavolta, S.; Gioffrè, M.; Focarete, M. L.; Gualandi, C.; Foroni, L.; Bigi, A. Electrospun Gelatin Nanofibers: Optimization of Genipin Cross-Linking to Preserve Fiber Morphology after Exposure to Water. *Acta Biomater.* **2011**, *7* (4), 1702−1709.
(108) Brenner, E. K.; Schiffman, J. D.; Thompson, E. A.; Toth, L. J.; Schauer, C. L. Electrospinning of Hyaluronic Acid Nanofibers from Aqueous Ammonium Solutions. *Carbohydr. Polym.* **2012**, *87* (1), 926−929.
(109) Memic, A.; Colombani, T.; Eggermont, L. J.; Rezaeeyazdi, M.; Steingold, J.; Rogers, Z. J.; Navare, K. J.; Mohammed, H. S.; Bencherif, S. A. Latest Advances in Cryogel Technology for Biomedical Applications. *Adv. Ther.* **2019**, *2* (4), 1800114.
(110) Wu, X.; Black, L.; Santacana-Laffitte, G.; Patrick, C. W., Jr Preparation and Assessment of Glutaraldehyde-crosslinked Collagen−Chitosan Hydrogels for Adipose Tissue Engineering. *J. Biomed. Mater. Res. Part A* **2007**, *81A* (1), 59−65.
(111) Grenier, J.; Duval, H.; Barou, F.; Lv, P.; David, B.; Letourneur, D. Mechanisms of Pore Formation in Hydrogel Scaffolds Textured by Freeze-Drying. *Acta Biomater.* **2019**, *94*, 195−203.
(112) Stokols, S.; Tuszynski, M. H. The Fabrication and Characterization of Linearly Oriented Nerve Guidance Scaffolds for Spinal Cord Injury. *Biomaterials* **2004**, *25* (27), 5839−5846.
(113) Coogan, K. R.; Stone, P. T.; Sempertegui, N. D.; Rao, S. S. Fabrication of Micro-Porous Hyaluronic Acid Hydrogels through Salt Leaching. *Eur. Polym. J.* **2020**, *135*, 109870.
(114) Burger, D.; Beaumont, M.; Rosenau, T.; Tamada, Y. Porous Silk Fibroin/Cellulose Hydrogels for Bone Tissue Engineering via a Novel Combined Process Based on Sequential Regeneration and Porogen Leaching. *Mol. 2020, Vol. 25, Page 5097* **2020**, *25* (21), 5097.
(115) Testouri, A.; Honorez, C.; Barillec, A.; Langevin, D.; Drenckhan, W.; Orsay, U. M. R. Highly Structured Foams from Chitosan Gels. *Macromolecules* **2010**, *43* (14), 6166−6173.
(116) Haung, S. M.; Lin, Y. T.; Liu, S. M.; Chen, J. C.; Chen, W. C. In Vitro Evaluation of a Composite Gelatin−Hyaluronic Acid−Alginate Porous Scaffold with Different Pore Distributions for Cartilage Regeneration. *Gels 2021, Vol. 7, Page 165* **2021**, *7* (4), 165.
(117) Babaei, J.; Mohammadian, M.; Madadlou, A. Gelatin as Texture Modifier and Porogen in Egg White Hydrogel. *Food Chem.* **2019**, *270*, 189−195.
(118) Sokic, S.; Christenson, M.; Larson, J.; Papavasiliou, G. In Situ Generation of Cell-Laden Porous MMP-Sensitive PEGDA Hydrogels by Gelatin Leaching. *Macromol. Biosci.* **2014**, *14* (5), 731−739.
(119) Dehghani, F.; Fathi, A.*Gels Handbook: Fundamentals, Properties and Applications*; Demirci, U., Khademhosseini, A., Eds.; World Scientific, 2016; Vol. *1*; DOI: 10.1142/9490.

https://doi.org/10.1021/acs.langmuir.2c02253
Langmuir XXXX, XXX, XXX−XXX

(120) Abbasian Chaleshtari, Z.; Zhou, M.; Foudazi, R. Nanoemulsion Polymerization and Templating: Potentials and Perspectives. *J. Appl. Phys.* **2022**, *131* (15), 150902.
(121) Dušková-Smrčková, M.; Zavřel, J.; Bartoš, M.; Kaberova, Z.; Filová, E.; Zárubová, J.; Šlouf, M.; Michálek, J.; Vampola, T.; Kubies, D. Communicating Macropores in PHEMA-Based Hydrogels for Cell Seeding: Probabilistic Open Pore Simulation and Direct Micro-CT Proof. *Mater. Des.* **2021**, *198*, 109312.
(122) Dragan, E. S.; Dinu, M. V. Advances in Porous Chitosan-Based Composite Hydrogels: Synthesis and Applications. *React. Funct. Polym.* **2020**, *146*, 104372.
(123) Babić Radić, M. M.; Filipović, V. V.; Vukomanović, M.; Runić, J. N.; Tomić, S. L. Degradable 2-Hydroxyethyl Methacrylate/Gelatin/Alginate Hydrogels Infused by Nanocolloidal Graphene Oxide as Promising Drug Delivery and Scaffolding Biomaterials. *Gels* **2022**, *8* (1), 22.
(124) Wang, Y.; Qian, J.; Zhao, N.; Liu, T.; Xu, W.; Suo, A. Novel Hydroxyethyl Chitosan/Cellulose Scaffolds with Bubble-like Porous Structure for Bone Tissue Engineering. *Carbohydr. Polym.* **2017**, *167*, 44−51.
(125) Plieva, F. M.; Kirsebom, H.; Mattiasson, B. Preparation of Macroporous Cryostructurated Gel Monoliths, Their Characterization and Main Applications. *J. Sep. Sci.* **2011**, *34* (16−17), 2164−2172.
(126) Carvalho, B. M. A.; Da Silva, S. L.; Da Silva, L. H. M.; Minim, V. P. R.; Da Silva, M. C. H.; Carvalho, L. M.; Minim, L. A. Cryogel Poly (Acrylamide): Synthesis, Structure and Applications. *Sep. Purif. Rev.* **2014**, *43* (3), 241−262.
(127) Saadat, Y.; Imran, O. Q.; Osuji, C. O.; Foudazi, R. Lyotropic Liquid Crystals as Templates for Advanced Materials. *J. Mater. Chem. A* **2021**, *9*, 21607−21658.
(128) Langevin, D. Microemulsions and Liquid Crystals. *Mol. Cryst. Liq. Cryst.* **1986**, *138* (1), 259−305.
(129) DePierro, M. A.; Carpenter, K. G.; Guymon, C. A. Influence of Polymerization Conditions on Nanostructure and Properties of Polyacrylamide Hydrogels Templated from Lyotropic Liquid Crystals. *Chem. Mater.* **2006**, *18* (23), 5609−5617.
(130) Bennett, D. J.; Burford, R. P.; Davis, T. P.; Tilley, H. J. Synthesis of Porous Hydrogel Structures by Polymerizing the Continuous Phase of a Microemulsion. *Polym. Int.* **1995**, *36* (3), 219−226.
(131) Hentze, H.-P.; Kaler, E. W. Polymerization of and within Self-Organized Media. *Curr. Opin. Colloid Interface Sci.* **2003**, *8* (2), 164−178.
(132) Mann, S.; Burkett, S. L.; Davis, S. A.; Fowler, C. E.; Mendelson, N. H.; Sims, S. D.; Walsh, D.; Whilton, N. T. Sol−Gel Synthesis of Organized Matter. *Chem. Mater.* **1997**, *9* (11), 2300−2310.
(133) Qavi, S.; Bandegi, A.; Firestone, M.; Foudazi, R. Polymerization in Soft Nanoconfinements of Lamellar and Reverse Hexagonal Mesophases. *Soft Matter* **2019**, *15* (41), 8238−8250.
(134) Williams, J. M.; Wrobleski, D. A. Spatial Distribution of the Phases in Water-in-Oil Emulsions. Open and Closed Microcellular Foams from Cross-Linked Polystyrene. *Langmuir* **1988**, *4* (3), 656−662.
(135) Zhou, M.; Foudazi, R. Effect of Cosurfactant on Structure and Properties of Polymerized High Internal Phase Emulsions (PolyHIPEs). *Langmuir* **2021**, *37* (26), 7907−7918.
(136) Menner, A.; Bismarck, A. New Evidence for the Mechanism of the Pore Formation in Polymerising High Internal Phase Emulsions or Why PolyHIPEs Have an Interconnected Pore Network Structure. *Macromol. Symp.* **2006**, *242* (1), 19−24.
(137) Wu, R.; Menner, A.; Bismarck, A. Tough Interconnected Polymerized Medium and High Internal Phase Emulsions Reinforced by Silica Particles. *J. Polym. Sci. Part A Polym. Chem.* **2010**, *48* (9), 1979−1989.
(138) Kovačič, S.; Štefanec, D.; Krajnc, P. Highly Porous Open-Cellular Monoliths from 2-Hydroxyethyl Methacrylate Based High Internal Phase Emulsions (HIPEs): Preparation and Void Size Tuning. *Macromolecules* **2007**, *40* (22), 8056−8060.
(139) Ikem, V. O.; Menner, A.; Horozov, T. S.; Bismarck, A. Highly Permeable Macroporous Polymers Synthesized from Pickering Medium and High Internal Phase Emulsion Templates. *Adv. Mater.* **2010**, *22* (32), 3588−3592.
(140) Barkan-Öztürk, H.; Menner, A.; Bismarck, A. Emulsion-Templated Macroporous Polymer Micromixers. *Ind. Eng. Chem. Res.* **2021**, *60* (39), 14013−14025.
(141) Raj, W. R. P.; Sasthav, M.; Cheung, H. M. Formation of Polymeric Foams from Aqueous Foams Stabilized Using a Polymerizable Surfactant. *J. Appl. Polym. Sci.* **1993**, *49* (8), 1453−1470.
(142) Colosi, C.; Costantini, M.; Barbetta, A.; Pecci, R.; Bedini, R.; Dentini, M. Morphological Comparison of PVA Scaffolds Obtained by Gas Foaming and Microfluidic Foaming Techniques. *Langmuir* **2013**, *29* (1), 82−91.
(143) Lee, K.-Y.; Wong, L. L. C.; Blaker, J. J.; Hodgkinson, J. M.; Bismarck, A. Bio-Based Macroporous Polymer Nanocomposites Made by Mechanical Frothing of Acrylated Epoxidised Soybean Oil. *Green Chem.* **2011**, *13* (11), 3117−3123.
(144) Jalalian, M.; Jiang, Q.; Birot, M.; Deleuze, H.; Woodward, R. T.; Bismarck, A. Frothed Black Liquor as a Renewable Cost Effective Precursor to Low-Density Lignin and Carbon Foams. *React. Funct. Polym.* **2018**, *132*, 145−151.
(145) Barbetta, A.; Rizzitelli, G.; Bedini, R.; Pecci, R.; Dentini, M. Porous Gelatin Hydrogels by Gas-in-Liquid Foam Templating. *Soft Matter* **2010**, *6* (8), 1785−1792.
(146) Barbetta, A.; Carrino, A.; Costantini, M.; Dentini, M. Polysaccharide Based Scaffolds Obtained by Freezing the External Phase of Gas-in-Liquid Foams. *Soft Matter* **2010**, *6* (20), 5213−5224.
(147) Lau, T. H. M.; Wong, L. L. C.; Lee, K.-Y.; Bismarck, A. Tailored for Simplicity: Creating High Porosity, High Performance Bio-Based Macroporous Polymers from Foam Templates. *Green Chem.* **2014**, *16* (4), 1931−1940.
(148) Lober, F. Entwicklung Und Bedeutung von Treibmitteln Bei Der Herstellung von Schaumstoffen Aus Kautschuk Und Kunststoffen. *Angew. Chem.* **1952**, *64* (3), 65−76.
(149) Andrieux, S.; Drenckhan, W.; Stubenrauch, C. Highly Ordered Biobased Scaffolds: From Liquid to Solid Foams. *Polymer (Guildf)* **2017**, *126*, 425−431.
(150) Costantini, M.; Colosi, C.; Mozetic, P.; Jaroszewicz, J.; Tosato, A.; Rainer, A.; Trombetta, M.; Święszkowski, W.; Dentini, M.; Barbetta, A. Correlation between Porous Texture and Cell Seeding Efficiency of Gas Foaming and Microfluidic Foaming Scaffolds. *Mater. Sci. Eng., C* **2016**, *62*, 668−677.
(151) van der Net, A.; Gryson, A.; Ranft, M.; Elias, F.; Stubenrauch, C.; Drenckhan, W. Highly Structured Porous Solids from Liquid Foam Templates. *Colloids Surfaces A Physicochem. Eng. Asp.* **2009**, *346* (1−3), 5−10.
(152) Costantini, M.; Colosi, C.; Jaroszewicz, J.; Tosato, A.; Święszkowski, W.; Dentini, M.; Garstecki, P.; Barbetta, A. Microfluidic Foaming: A Powerful Tool for Tailoring the Morphological and Permeability Properties of *Sponge-like* Biopolymeric Scaffolds. *ACS Appl. Mater. Interfaces* **2015**, *7* (42), 23660−23671.
(153) Chung, K.-Y.; Mishra, N. C.; Wang, C.-C.; Lin, F.-H.; Lin, K.-H. Fabricating Scaffolds by Microfluidics. *Biomicrofluidics* **2009**, *3* (2), 022403.
(154) Testouri, A.*Highly Structured Polymer Foams from Liquid Foam Templates Using Millifluidic Lab-on-a-Chip Techniques*; Université Paris Sud - Paris XI, 2012.
(155) Testouri, A.; Ranft, M.; Honorez, C.; Kaabeche, N.; Ferbitz, J.; Freidank, D.; Drenckhan, W. Generation of Crystalline Polyurethane Foams Using Millifluidic Lab-on-a-Chip Technologies. *Adv. Eng. Mater.* **2013**, *15* (11), 1086−1098.
(156) Salonen, A.; Lhermerout, R.; Rio, E.; Langevin, D.; Saint-Jalmes, A. Dual Gas and Oil Dispersions in Water: Production and Stability of Foamulsion. *Soft Matter* **2012**, *8* (3), 699−706.
(157) Boettcher, A.; Hensen, H.; Seipel, W.; Tesmann, H.*Foaming Emulsions*. US5656200A, 1997. DOI: 10.1016/j.atmos-env.2011.03.055.
(158) Schneider, M.; Zou, Z.; Langevin, D.; Salonen, A. Foamed Emulsion Drainage: Flow and Trapping of Drops. *Soft Matter* **2017**, *13* (22), 4132−4141.

https://doi.org/10.1021/acs.langmuir.2c02253
Langmuir XXXX, XXX, XXX−XXX

(159) Mensire, R.; Lorenceau, E. Stable Oil-Laden Foams: Formation and Evolution. *Adv. Colloid Interface Sci.* **2017**, *247*, 465−476.
(160) Mirzaei, B. E.; Ramazani, A.; Shafiee, M.; Danaei, M. Studies on Glutaraldehyde Crosslinked Chitosan Hydrogel Properties for Drug Delivery Systems. *Int. J. Polym. Mater. Polym. Biomater.* **2013**, *62* (11), 605−611.
(161) Andrieux, S.; Medina, L.; Herbst, M.; Berglund, L. A.; Stubenrauch, C. Monodisperse Highly Ordered Chitosan/Cellulose Nanocomposite Foams. *Compos. Part A Appl. Sci. Manuf.* **2019**, *125*, 105516.
(162) Ceccaldi, C.; Bushkalova, R.; Cussac, D.; Duployer, B.; Tenailleau, C.; Bourin, P.; Parini, A.; Sallerin, B.; Girod Fullana, S. Elaboration and Evaluation of Alginate Foam Scaffolds for Soft Tissue Engineering. *Int. J. Pharm.* **2017**, *524* (1−2), 433−442.

https://doi.org/10.1021/acs.langmuir.2c02253
Langmuir XXXX, XXX, XXX−XXX